Applied Catalysis A, General 691 (2025) 120088

Contents lists available at ScienceDirect

Applied Catalysis A, General

journal homepage: www.elsevier.com/locate/apcata

Hydrotalcite-catalyzed methylation of isosorbide via dimethyl carbonate: Influence of the catalyst on the reaction mechanism

María José Ginés-Molina [a], José Santamaría-González [a,b], Pedro Maireles-Torres [a,b], Juan A. Cecilia [a,b], Rafael Luque [c,d], Manuel López-Granados [e], Giacomo Trapasso [f], Fabio Aricò [f], Juan Soto [g], Ramón Moreno-Tost [a,b,*]

[a] Universidad de Málaga, Departamento de Química Inorgánica, Cristalografía y Mineralogía, Facultad de Ciencias, Campus de Teatinos s/n, Málaga 29071, Spain
[b] Instituto de Investigación en Biorrefinerías "I3B", Universidad de Málaga, Facultad de Ciencias, Campus de Teatinos s/n, Málaga 29071, Spain
[c] Peoples Friendship University of Russia (RUDN University), 6 Miklukho Maklaya str., Moscow 117198, Russian Federation
[d] Universidad ECOTEC, Km 13.5 Samborondón, Samborondón, EC092302, Ecuador
[e] EQS Group (Sustainable Energy and Chemistry Group), Institute of Catalysis and Petrochemistry (ICP-CSIC), C/Marie Curie 2, Madrid 28049, Spain
[f] Department of Environmental Science, Informatics and Statistics, Ca' Foscari University of Venice, Campus Scientifico, Via Torino 155, Venezia Mestre 30172, Italy
[g] Department of Physical Chemistry, Faculty of Sciences, University of Málaga, Málaga E-29071, Spain

ARTICLE INFO

Keywords:
Hydrotalcite
Dimethyl carbonate
Isosorbide
Dimethyl isosorbide
Flow chemistry
DFT analysis

ABSTRACT

This work presents the results of the methylation of isosorbide to produce dimethyl isosorbide using dimethyl carbonate as methylating agent and reaction medium and a MgAl mixed oxide derived from the calcination of a commercial hydrotalcite as basic catalyst. This reaction was carried out using three types of reactors: a continuous liquid flow reactor and two batch reactors, the first one working at autogenous pressure and the other one at atmospheric pressure. The best results were achieved for the atmospheric pressure reactor, with the dimethyl isosorbide yield being 100 % at 110 ºC, after 8 h. Under these experimental conditions, the catalyst showed a loss of selectivity towards dimethyl isosorbide with consecutive catalytic cycles, reaching approximately 50 % dimethyl isosorbide yield after 5 catalytic cycles, but maintaining the isosorbide conversion at 100 %. The reaction mechanism most probably relies on the cooperation between the catalyst and the dimethyl carbonate. With the help of computational studies, it has been demonstrated that the adsorption of dimethyl carbonate on the catalyst takes place through the carbonyl group and that it adsorbs on either Mg^{2+} or Al^{3+} ions. Finally, the assignation of the FTIR bands corresponding to the adsorbed dimethyl carbonate species revealed that it undergoes a surface reaction, leading to the formation of both methoxide and monomethyl carbonate adsorbed species. The presence of such species was identified as responsible for the changing pattern selectivity of the reaction during the reutilization of the catalyst.

1. Introduction

Starting from the nineties, the development of Green Chemistry has boosted the research for processes, materials, reagents and products that are environmentally benign, generate less waste, consume less energy and are more atom efficient [1]. The final scope is to synthesize target compounds in high yields, shorter times and with milder reaction conditions via green(er) approaches [2].

A poignant example of this paradigm is the synthesis of dimethyl carbonate (DMC). DMC - the smallest representative of the organic carbonates - was industrially prepared by a phosgene route until the mid-80's of the last century, when this synthesis was replaced by greener ones such as i) the oxidative carbonylation of methanol using oxygen as oxidant (Enichem, Italy) or ii) the UBE process (Japan), in which NO_x is used as oxidant [3].

DMC has found a wide range of applications in areas such as pharmaceuticals, lithium-based batteries, coatings, in the polycarbonate industry, etc. [3–5]. Moreover, DMC is considered a green reagent [6] in substitution of hazardous and highly toxic compounds, such as phosgene for carboxymethylation reactions, and dimethyl sulphate or methyl

* Corresponding author at: Universidad de Málaga, Departamento de Química Inorgánica, Cristalografía y Mineralogía, Facultad de Ciencias, Campus de Teatinos s/n, Málaga 29071, Spain
E-mail address: rmtost@uma.es (R. Moreno-Tost).

https://doi.org/10.1016/j.apcata.2024.120088
Received 22 October 2024; Received in revised form 29 November 2024; Accepted 20 December 2024
Available online 24 December 2024

halides for methylation reactions [7]. In fact, depending on the substrate and reaction conditions, DMC can act as methylating agent [8], when the methyl groups (soft electrophile) are attacked by a soft nucleophile, or as a carboxymethylating agent [9], when the carbonyl group (hard electrophile) is attacked by a hard nucleophile, according to Pearson's Hard-Soft Acid-Base theory. It should be noted that the methylation reaction typically requires higher temperatures (T > 150 °C) compared to methoxycarbonylation reactions (T = 90 °C).

Tundo et al. conducted an in-depth study on the methylation of primary, secondary and tertiary alcohols with DMC [8]. When primary alcohols, 1-octanol and benzyl alcohol, were employed as substrates in the presence of weak bases (K_2CO_3), the selective formation of the methoxycarbonylated products was observed. However, when calcined hydrotalcite or basic alumina were tested as catalysts, the methyl derivatives of these alcohols were obtained as main products. The authors proposed that the formation of methyl derivatives proceeded via a two steps route, where first the transesterification between DMC and the alcohol took place, followed by a decarboxylation of the methyl carbonate to yield the methyl ether. Despite the heterogeneous catalytic nature of the reaction, the role of the catalyst in both the transesterification and decarboxylation reactions was not addressed in this study. When secondary or tertiary alcohols were examined, elimination products were mainly formed, as expected.

Isosorbide (IS) is a cyclic sugar derived from D-sorbitol that presents a peculiar V-shaped structure (Scheme S1) in which all the oxygens are in β position to each other [10]. The secondary alcohols of the IS are labeled differently: the *endo* hydroxyl group points toward the V-shaped cavity, while the *exo* hydroxyl group points outward [7]. A strong intramolecular hydrogen bond exists between the *endo* alcohol and the oxygen atom of the opposite tetrahydrofuran ring. As a result, the two hydroxylic moieties have a different reactivity, indeed the *endo* hydroxyl group resulted more easily methylated than the *exo* one. The rigidity of the structure has made IS a viable alternative to bisphenol A in the synthesis of polycarbonates [11] and for the synthesis of polyurethanes [12]. Polycarbonates derived from IS showed improved properties, such as UV stability and non-toxic nature compared to the polycarbonates derived from the bisphenol A route [13]. An additional application of IS is in the synthesis of the nitrate derivative used as medicines for heart diseases which also has direct applications for treating glaucoma and brain hypertension [14,15].

Another interesting compound derived from IS is its methylated derivative, called dimethyl isosorbide (DMI). DMI is an interesting green solvent, with a high boiling point (236 ºC) and negligible bioaccumulation [16]. These properties make it suitable for use in cosmetic and pharmaceutical formulations [17]. DMI is a polar molecule completely miscible with water, so it has also been described as a solvent for the organosolv pre-treatment of biomass [16] and for the preparation of ultrafiltration membranes [18].

The synthesis of DMI can be achieved by means of the methyl halide route, or by exploiting the reactivity of DMC. The latter approach was proposed by Tundo et al. [10], who synthesized DMI in quantitative yields when an excess of sodium methoxide was used as a base, at the reflux temperature of DMC for 20 hours. In this process, methoxide anions are generated as by-products in the methylation reaction, so the base could also in principle be used in catalytic amount. DMI was prepared in 86 % yield when a calcined commercially available hydrotalcite was used as catalyst in a 1:1 (cat:IS) weight ratio at 200 ºC for 20 hours [19]. However, the mechanism of the methylation of IS has never been fully elucidated when the heterogeneous catalysis approach has been carried out. Homogenous basic organocatalyst N-methyl pyrrolidine was also efficiently used for the preparation of DMI, as well as for the methylation of IS epimers, isoidide and isomannide, in almost quantitative yield. The reactions were conducted in autoclave at 200 °C for 12 hours and some scale-up tests were reported up to 10 g of DMI [17]. A more recent approach to DMI focused on the use of a heterogeneous acid catalyst [20]. In this case, the reaction conditions were harsher than the basic ones, resulting in a DMI yield of ca 80 % at 200 ºC, whereas a high autogenous pressure was caused by the acid-catalyzed decomposition of DMC to CO_2 and methanol.

Alternative procedures for the methylation of IS include the use of methanol as methylating agent in the presence of polyacids, zeolites and zirconia-based catalysts [21]. Other reported synthetic approaches encompass i) methylphosphates in the presence of Lewis acid catalysts [22] and ii) 1,2-dimethoxyethane used as reagent/solvent in the presence of heteropolyacids [23].

From these premises, the aim of this work is to further investigate the synthesis of DMI via DMC chemistry, employing a calcined hydrotalcite as catalyst, with special emphasis on the reaction mechanism, the effect of experimental conditions and the role of both DMC and the catalyst. The reaction was carried out in three different systems: a continuous flow liquid reactor and two batch reactors, one operating at autogenous pressure and the other at atmospheric pressure. The reaction mechanism was evaluated by FTIR spectroscopy analysis of the adsorption of DMC on the surface of the catalyst, by computational studies and by the evolution of the reaction intermediates along the reaction. Furthermore, recovery and recycling of the catalyst were also addressed, including its characterization after the reaction.

2. Materials and methods

2.1. Materials

Isosorbide (IS; 98 %, Sigma-Aldrich), dimethyl carbonate (DMC; 99 %, Sigma-Aldrich), dimethyl isosorbide (DMI; 99.9 %, Sigma-Aldrich), methanol (MeOH; VWR, HPLC gradient grade), cyclopentyl methyl ether (CPME; 99.9 %, Sigma-Aldrich), dimethylformamide (DMF; 99.9 %, Sigma-Aldrich) hydrotalcite (HT; $Mg_6Al_2(OH)_{16}](CO_3)\cdot 4\ H_2O$; 19 % Mg, 1.2 % Al, Sigma-Aldrich), magnesium oxide (MgO; 98 %, Fluka Analytical), alumina (Al_2O_3; Alfa Aesar), nitrogen (N_2; 99,9999 %, Air Liquide).

2.2. Catalytic reaction

2.2.1. Batch reactors

In all the tests carried out in this work, prior to the catalytic reaction, the hydrotalcite (HT) was activated in an oven at 450 ºC with a ramp of 10 ºC/min in order to generate the $MgAlO_x$ mixed oxide, active in the reaction. For the reaction at **autogenous pressure** conditions, the activated catalyst was poured into the glass liner of the Parr® reactor (Parr Instrument Company, Model 4560 Mini Bench Top Reactors) containing the solution of IS in DMC (0.02 M). The capacity of the glass liner was of 100 mL and the volume of the dissolution was fixed at 56 mL. The pressure and temperature of the reactor was monitored by a 4848 Reactor Controller (Parr Instrument Company).

For the reaction at **atmospheric pressure**, the activated HT was poured in a Pyrex glass batch reactor with PTFE stopper, with a capacity of 20 mL (dimensions of 150 mm×24 mm ø) and magnetic stirring (Cross shape stirring bar, 10 mm, Radleys®). The reactor was charged with 5 mL of IS solution (0.02 M) and introduced into a reaction station type Carousel 12 plus (Radleys®), which is connected to a cooling system with recirculation of ethylene glycol and water mixture.

Different reaction variables were modified for both systems, such as the reaction temperature, reaction time and catalyst/IS mass ratio. At the end of the reaction, the catalyst was filtered under vacuum to separate the catalyst from the reaction medium and then dried in an oven at 60 °C for 24 hours. For reuse tests, the catalyst was decanted into the reactor and the reaction solution was removed, leaving the catalyst in the reactor. Then, a new fresh IS solution was added and the reaction was restarted.

The reaction products were then analyzed by a gas chromatograph (Shimadzu model GC 14 A), equipped with Flame Ionization Detector (GC-FID) and a TBR-14 fused silica capillary column. Tetralin was used

as internal standard and added to reaction medium after the reaction. The IS conversion and selectivities to the different compounds were calculated from the following formulas:

$$Conversion(\%) = \frac{(mol\ isosorbide)_c}{(mol\ isosorbide)_i}\ x\ 100$$

$$Selectivity_i\ (\%) = \frac{(mol\ product)_i}{(mol\ isosorbide)_c}\ x\ 100$$

$$Yield_i\ (\%) = Conversion\ x\ Selectivity_i$$

Where, $(mol\ IS)_i$ stands for initial amount of IS and $(mol\ IS)_c$ refers to mol of converted IS. The Figure S1 shows a typical chromatogram of the reaction. The carbon balance was calculated as the sum of the detected compounds yields.

2.2.2. Flow reactor

In this case, each reaction was performed with fresh activated HT. Firstly, the catalyst was activated in a muffle as described above and kept in contact with DMC at room temperature prior to reactor loading. The reaction was carried out in a Phoenix Flow Reactor (ThalesNano®). The activated HT was loaded in a 30 mm ThalesNano CatCart and transferred to the reactor oven, then, pure liquid DMC was passed through the catalytic bed until the DMC was collected at the reactor outlet, at which time the flow of DMC was changed to IS solution and the temperature was raised to the desired value. Samples were collected at various reaction times and analyzed by GC-FID, as previously mentioned.

2.3. Experimental techniques

CNH analysis was performed on a Leco TruSpec Micro CHNSO Elemental Analyzer. The thermal behavior of the samples before and after reaction was studied on a METTLER TOLEDO thermal analyzer model TGA/DSC 1 capable of simultaneously measuring TG and DSC values of samples up to 10 μg. The thermobalance is coupled to the outlet of a PFEIFFER VACUUM mass spectrometer, model ThermoStar TM GSD 320. The measuring range is 1–200 amu. The tests were carried out in 70 μl Al_2O_3 crucibles in the temperature range 30–900 °C, with an air flow of 50 mL/min and a heating rate of 10 °C/min. For the attenuated total reflectance infrared analysis (ATR-FTIR) of the samples, a Bruker Vertex70 FT-IR Spectrophotometer with a Golden Gate Single Reflection Diamond ATR System accessory was used. The samples were analyzed without pre-treatment. A standard spectral resolution of 4 cm^{-1} in the spectral range 4500–500 cm^{-1} was employed for the acquisition of the spectra, as well as 64 scans. The background in all cases was air. The surface composition of the samples was determined by the X-Ray photoelectron spectroscopy (XPS), which was performed on a Physical Electronics PHI 5700 spectrometer with non-monochromatic Mg K_α radiation (300 W, 15 kV, 1253.6 eV std) and a multichannel hemispherical detector. All the narrow scan spectra were recorded at a step energy of 29.35 eV and an analysis area of 720 μm. The energy scale of the spectrometer was calibrated using the Cu $2p_{3/2}$, Ag $3d_{5/2}$ and Au 4 $f_{7/2}$ photoelectron lines at the binding energies of 932.7, 368.3 and 84.0 eV, respectively. ^{1}H MAS NMR (magic angle spinning nuclear magnetic resonance, ^{1}H-ss NMR) spectra were recorded at room temperature in an AVANCEIII HD 600 (Bruker AXS) spectrometer, using a triple resonance DVT probe of 2.5 mm at a spinning rate of 25 kHz. The magnetic field was 14.1 T, corresponding to a ^{1}H resonance frequency of 600.09 MHz. The ^{1}H chemical shifts are referenced to adamantane. ^{1}H-ss NMR spectra were recorded with a pulse of width of 2 us, a power of pulse of 49 W, and 3-s delay with and summing up 64 scans. ^{13}C CPMAS NMR (magic angle spinning nuclear magnetic resonance, ^{13}C-ss NMR) spectra were registered at room temperature, using a triple resonance CPMAS probe of 4 mm at a spinning rate of 13 kHz. The magnetic field was 14.1 T, corresponding to a ^{13}C resonance frequency of 150.91 MHz. The ^{13}C chemical shifts are referenced to adamantane. ^{13}C-ss NMR spectra were recorded with a contact time of 2 ms, a power of pulse of 155 W, and 3-s delay with and summing up 7000 scans.

The adsorption of DMC, or MeOH on the activated hydrotalcite was followed by FTIR analysis. The experiments were carried out in a glass line vacuum by contacting DMC or MeOH vapours on a wafer of activated HT. So, before adsorption, the activated hydrotalcite was evacuated overnight at 450 ºC in the glass line vacuum, then the temperature was lowered to the chosen one and DMC was allowed to adsorb on the surface of the catalyst. Prior to adsorption, a spectrum of the evacuated catalyst was recorded as a blank and subtracted from the following spectra. FTIR spectra of adsorbed species were recorded on a Shimadzu 8300 FTIR spectrometer at a resolution of 4 cm^{-1}. Each spectrum was averaged over 128 scans. Self-supporting wafers of hydrotalcite were placed in a vacuum cell with greaseless stopcocks and CaF_2 windows.

The description of both textural and acidity-basicity analysis can be found in the Supplementary Information

2.4. Computational analysis

The interactions of DMC with MgAl mixed oxides, as well as the IR spectra of both isolated and adsorbed species, have been studied by means of Density Functional Theory (DFT), which is demonstrated to be a good tool to study metal-organic adsorbate interactions [24]. To reach this end, the hybrid exchange-correlation functional M06–2X [25] was applied, that yields good numerical predictions of thermodynamic properties for organic and inorganic molecular systems [25,26]. The def2-TZVPP basis sets [27] have been applied to all of the atoms, which form the system under study in conjunction with the empirical dispersion correction of Grimme [28].

The electronic structure calculations were carried out with the program GAUSSIAN16 [29]. Adsorption energies were determined with the standard expressions of Statistical Thermodynamics. Molecular geometries were analyzed with the help of the MacMolPlt [30] and MOLDEN [31] graphical programs. The assignment of the observed bands of the spectra has been performed through the vibrational analysis in internal coordinates according with the GF method of Wilson [32–34].

3. Results and discussion

The catalytic activity of $MgAlO_x$ mixed oxide derived from a commercial hydrotalcite (HT) was evaluated in the methylation of IS with DMC, which was employed as solvent and reagent. Both hydrotalcite and $MgAlO_x$ mixed oxide have been previously characterized and the main physicochemical properties already reported in the literature [35]. It must be emphasized that, in the present work, only the characterization information necessary to understand the catalytic performance of both HT and $MgAlO_x$ mixed oxides has been used.

The main objective of this work is to unravel the mechanism behind the methylation reaction of IS with DMC, when using a basic solid catalyst. For this purpose, two discontinuous reactors (autogenous and atmospheric pressure) and one continuous liquid flow reactor were used. Different experimental conditions were evaluated for each reactor and the adsorption of both DMC and MeOH on the HT were studied in order to elucidate the evolution of the spectral features during the reaction, so to better understand the reaction mechanism.

The reaction (Scheme 1) of IS with DMC comprises eight different compounds: two monocarboxymethyl compounds (MC), one dicarboxymethyl compound (DC), two carboxymethyl/methyl compounds (MCE), two monomethyl compounds (MMI) and the desired dimethyl derivative (DMI) [10].

In this study, the MC and MCE intermediates were treated as the corresponding mixtures of isomers, since no attempt was made to obtain the pure compounds. It should be also pointed out that all the methoxycarbonylation reactions leading to DC, MC and MCE occur in

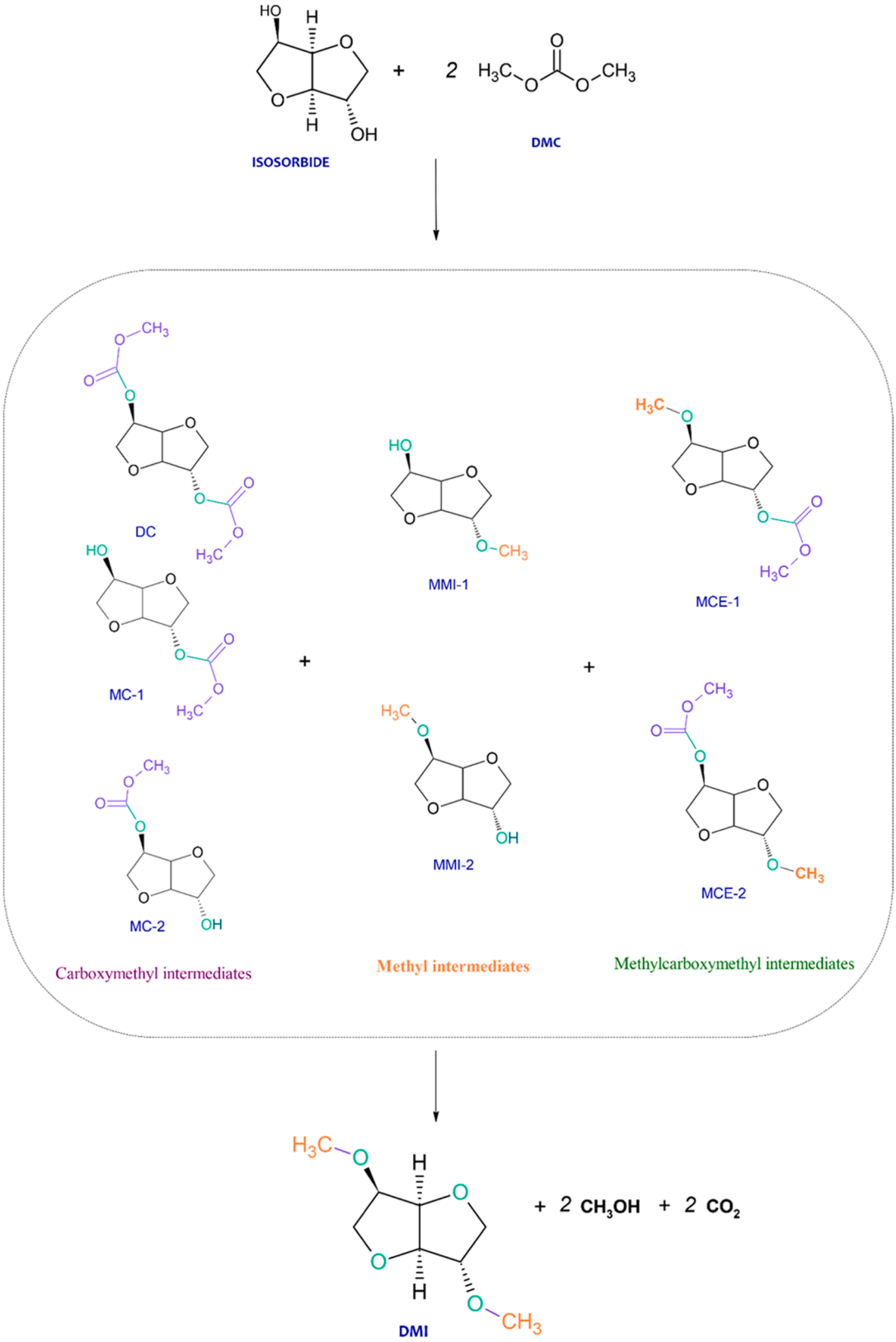

Scheme 1. Products evolving from the reaction of IS with DMC.

thermodynamic equilibrium, whereas the methyl derivatives (MMI and DMI) are formed via kinetically driven reactions. In the experiments herein conducted, the presence of these compounds was confirmed by GC-MS analysis. The pure compounds MC, DC and MCE (as mixtures) were prepared according to the procedures already reported in the literature [10].

3.1. Flow reaction in liquid phase

Reactions carried out in flow conditions are often faster than the corresponding ones performed in batch, resulting in improved energy consumption, time, and space efficiency [36]. The methylation of IS was conducted in a reactor that allows to maintain the reaction medium in the liquid phase, despite working at temperatures higher than the boiling point of the solvent. This was achieved by increasing the pressure of the reactor to 15 bar and varying the temperature between 160 and 200 ºC. Under these conditions, it was observed that the IS conversion was complete for all the tested reaction temperatures and times (Fig. 1). However, the sum of product yields never reached 100 %, and, in some tests, the difference between the conversion and the sum of the yields was as high as 80 %. In addition, DMI yields decreased as the reaction progressed, even though the IS conversion was still quantitative, this issue is discussed in detail in the Supplementary Information. Moreover, in order to evaluate the influence of pressure on the catalytic performance, some studies were carried out in which the system pressure was varied. For these experiments, the flow rate was fixed at 0.3 mL/min, the temperature range was between 170 and 185 ºC and the pressure was increased from 15 to 25 bar at each temperature. This increase in pressure had a negligible effect on the IS conversion and selectivity pattern (Fig. 2S), so the pressure does not seem to play a key role in the reaction and it is only necessary to carry out the reaction in a liquid phase.

Increasing the temperature caused the DMI yield to rise from approximately 4 %, at 160 °C and 60 minutes, to 37 %, at 200 °C and 67 minutes. As the reaction progressed, it was observed that at higher temperature, the yield of DMI continued to decrease. For example, at 160 °C (Fig. 1a), the DMI yield is quite constant over time, but, at 200 °C (Fig. 1d), it decreases significantly. Indeed, it diminishes from 37 %, after 60 minutes, to 10 %, after 180 minutes. These changes in selectivity could be related to changes on the catalyst surface due to irreversible adsorption of compounds involved in the reaction. Another possibility is that some of the compounds formed are retained in the porous network of the catalyst and not released in the reaction stream, resulting in lower-than-expected compound yields. On the other hand, it should also be noted that the DMC is susceptible to decomposition in the presence of basic catalysts at high temperature, as shown by Fu et al. [37], forming CO_2 and MeOH which would be adsorbed on the surface of

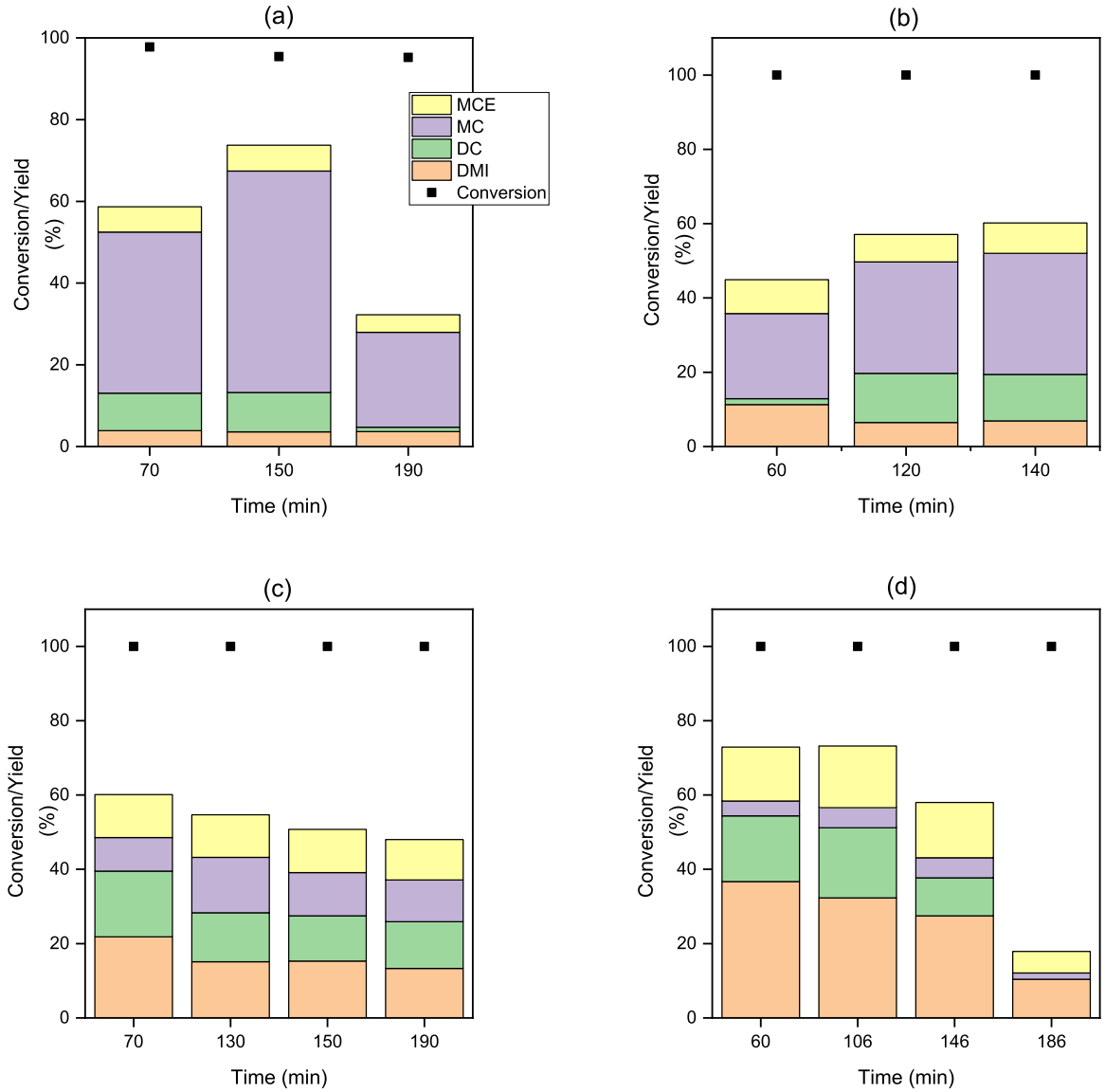

Fig. 1. IS conversion and product yields as function of temperature and feed flow. (a) Flow = 0.2 mL/min; T = 160 ºC; (b) Flow = 0.3 mL/min; T = 160 ºC; (c) Flow = 0.2 mL/min; T = 185 ºC; (d) Flow = 0.2 mL/min; T = 200 ºC. The other reaction conditions were maintained constant for the four experiments: P = 15 bar; mass catalyst (HT at 450 ºC) = 0.36 g; [IS] = 0.02 M.

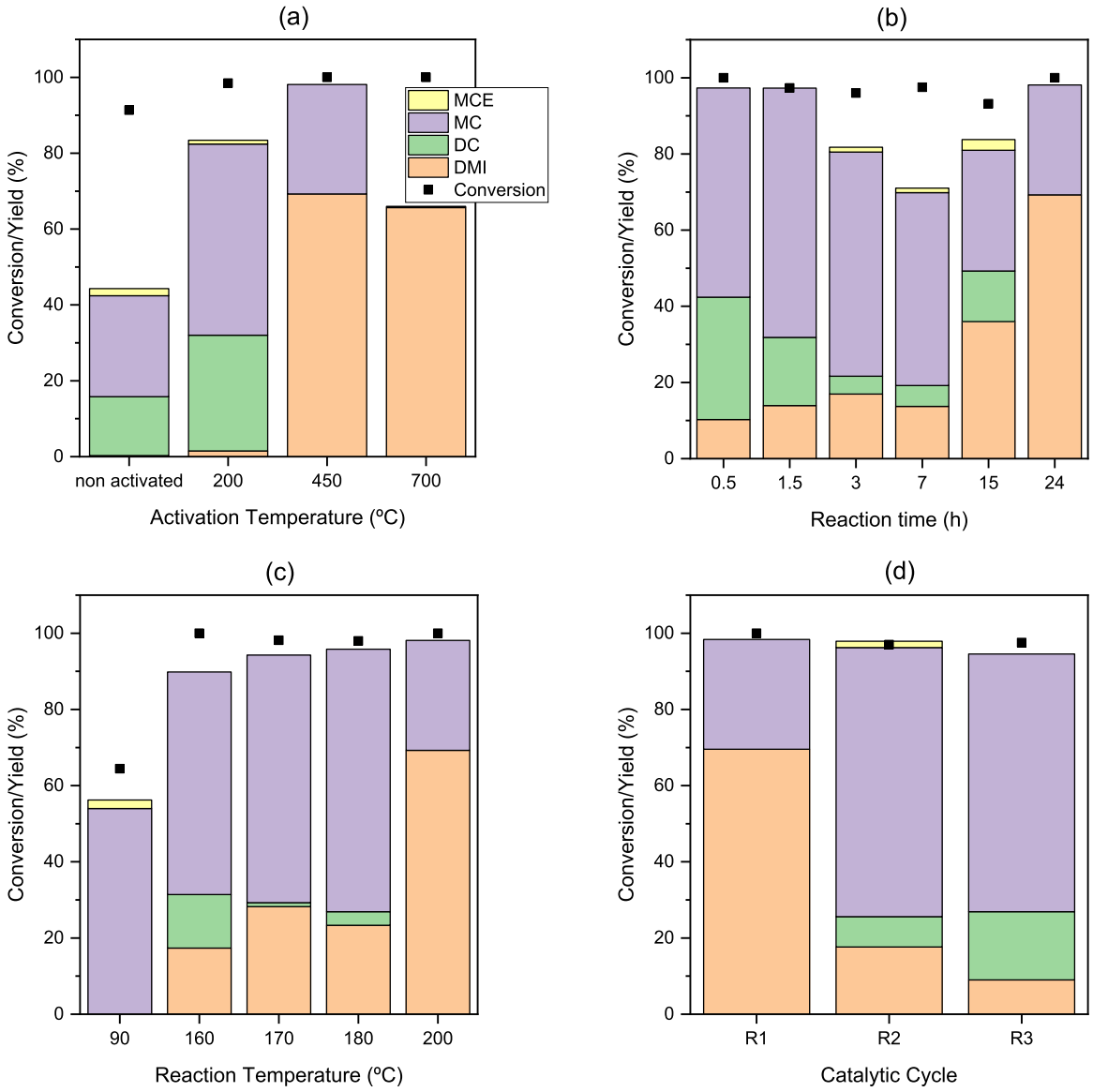

Fig. 2. IS conversion and product yields as a function of (a) activation temperature of HT; (b) reaction time; (c) reaction temperature and (d) reutilization cycles. Experimental conditions: [IS] = 0.02 M; cat:IS mass ratio = 3; HT activated at 450 ºC; autogenous pressure; reaction temperature = 200 ºC, except Fig. 2c; reaction time = 24 h, except Fig. 2b. Between each reutilization cycle, the catalyst was not reactivated.

the catalyst. The formation of CO_2 was visually confirmed by observing the formation of gas bubbles in the tubing at the outlet of the reactor, and the formation of bubbles became more pronounced as the temperature increased. Therefore, at higher temperatures, the catalyst was involved in both reactions: IS methylation and DMC decomposition.

The temperature also affected the selectivities toward the products formed. At 160 ºC, the formation of MC intermediates was favored, whereas, upon increasing the temperature, the selectivity was shifted to the methyl derivatives (MCE and DMI). This confirms that the $B_{Ac}2$ (bimolecular, base-catalyzed, acyl cleavage, nucleophilic substitution) mechanism is predominant at low temperatures and the $B_{Al}2$ (bimolecular, base-catalyzed, alkyl cleavage, nucleophilic substitution) mechanism (Scheme S3) becomes more significant as the temperature increases [38]. Therefore, the best conditions for achieving high DMI yields were those in which the temperature was high enough to favor the $B_{Al}2$ mechanism over the $B_{Ac}2$ one.

We can conclude that the DMI production from the flow reactor approach is not a good choice due to the rapid deactivation of the catalyst. Nevertheless, this system should not be completely discarded because we did not evaluate it with an acid catalyst. Therefore, new catalytic systems, probably based on acid catalysts [20], should be investigated in a flow reactor.

3.2. Batch conditions reaction

3.2.1. Reaction under autogenous pressure

The methylation of IS via DMC chemistry was also carried out in a hydrothermal reactor with a catalyst:IS mass ratio of 3 and a stirring rate of 200 rpm. This mass ratio was set from the non-activated HT, but, taking into account that the HT lost a 44 % of mass after the activation at 450 ºC [35], the actual catalyst:IS mass ratio was 1.7, taking into account that this is a basic catalyzed reaction, the concentration of basic sites of $MgAlO_x$ catalyst in the reactor is a key parameter to perform the methylation of IS. Considering the amount of basic sites (304 μmol·g^{-1}) added to the reactor and the mol of IS, the basic sites:IS molar ratio was 0.07. The rest of the parameters were adjusted to the specific reaction conditions. As reported in a previously published work [10], the HT was more efficient when activated at 450 °C (Fig. 2a). At lower activation

temperatures, the yield of DMI was negligible, while, when HT was activated at higher temperature (700 °C), the DMI yield did not show any improvement. Thus, after activating the HT at 450 °C and performing the reaction at 200 °C for 24 hours, the DMI yield was of 70 % (Fig. 2a), with MC being the only by-product formed.

The variation of the HT catalytic activity as a function of the activation temperature depends on its basic and textural properties [35]. Both the non-activated hydrotalcite and the hydrotalcite activated at 200 ºC were hydroxides, whose basicity was lower than that of the hydrotalcite activated at higher temperatures, which was a metal oxide. It was previously reported that, for the methylation reactions, strong bases are required [8,11], because weak bases led to the carboxymethylated compounds. In addition, the textural properties of the HT activated at 200 ºC or non-activated (Table S1) were worse than those of the HT activated at temperatures higher than 200 ºC.

Examining the evolution of reaction products at 200 ºC as the reaction progressed, it is interesting to highlight that DMI was already present in the first 30 minutes of reaction (Fig. 2b). Furthermore, the MC compound was the most abundant intermediate at any time, whereas DC emerged in the early stages of the reaction and then diminished at longer reaction times. The yield of MCE products was less than 3 % throughout the reaction, and monomethyl derivatives were not detected at any reaction time. Thus, it seems that the methoxycarbonylated intermediates were prone to evolve to the methylated compound. This could be ascribed to the decarboxylation at high temperatures to yield the methylether derivatives, as it was previously reported [8]. Moreover, this process could be favored by the fact that the formation of DMI from DC or MCE is not an equilibrium reaction, whereas the formation of carboxymethylated compounds from IS occurs under equilibrium conditions. Thus, when DMI is formed via decarboxylation, the equilibrium is shifted, leading to the consumption of the reaction intermediates.

When the reaction was performed at temperatures below 200 °C, both the IS conversion and selectivity to DMI were lower (Fig. 2c). As an example, at 90 °C (boiling temperature of DMC), the IS conversion was only 65 %, while the yield of DMI was zero and the only product detected was MC. As the reaction temperature was increased, the IS conversion and the DMI yield improved.

When the catalyst was reused (Fig. 2d), it was observed that, although the conversion of IS remained quantitative, the yield of DMI decreased significantly after three cycles and was only 9 % at the end of the 3rd cycle. In the latter recycling test, the most abundant products are those corresponding to the transesterification reaction (MC and DC). This fact suggests that the catalyst underwent some kind of change that modified its catalytic activity, preventing the selectivity of DMI from being maintained at the same level. This was confirmed by XPS analysis of the catalyst before and after reaction (Table S2 and Figure S2a). Indeed, before the reaction, the binding energies obtained for each of the elements (Table S2) coincide with those reported in the literature. Thus, the band corresponding to the O1s core level can be deconvoluted into two bands [39], the lower energy band being due to the oxide ion, while that a higher energy can be associated with the presence of surface hydroxyl groups. The presence of hydroxyl groups after the calcination of hydrotalcite at 450 ºC may be due to the fact that the mixed metal oxides were not kept in an inert atmosphere to prevent the adsorption of water, originating these groups, as it is also observed in the spectrum of the activated hydrotalcite (Figure S2b). Both the Mg2p and Al2p core level spectra correspond to Mg^{2+} and Al^{3+} ions in an oxidic environment [40–42]. The C1s band can be deconvoluted in several contributions that from lower to higher binding energies would correspond to C-C, C-O and carbonate [42–45]. After the reaction, all the analyzed core levels show significant changes. For the O1s, the band corresponding to the oxide ion disappears, the band ascribed to hydroxyl group slightly increased its intensity and a new band appears at 533.7 eV. which is associated with the O present in ether-type oxygen of ester molecules [41,45], such that found in DMC or carboxymethylated compounds. On the other hand, the Al2p and Mg2p core levels split into two bands, the lower energy bands being due to the corresponding ions in the oxygen environment, while the higher binding energy band ascribed to M-O-C bonds [41,46]. Therefore, after the reaction the catalyst surface is partially covered with organic moieties bonded to the metallic cations, this fact will be confirmed below. Considering that after 24 hours of reaction the sum of the products yields was close to 100 %, these species must have originated from DMC and not from IS or other reaction intermediates, otherwise the carbon balance would have been lower than 100 %.

3.2.2. *Reaction under atmospheric pressure*

After studying this reaction in a continuous flow reactor and in a discontinuous hydrothermal reactor, both requiring high pressures and temperatures, the methylation of IS under batch conditions, at atmospheric pressure and at lower temperature, was also investigated, still using the HT activated at 450 ºC as catalyst. This idea was based on previously reported studies [10] on the methylation of IS in the presence of sodium methoxide, at the boiling temperature of DMC (90 ºC), that led to DMI in almost quantitative yield, using a sodium methoxide:IS mass ratio of 1.1.

In our tests, the mass ratio between the activated hydrotalcite and the IS was set at 6.1, being the molar ratio between basic sites and IS of 0.3. Catalytic data showed the formation of carboxymethylated compounds (MC and DC), methyl-carboxymethylated compounds (MCE) and DMI. The monomethylated compounds (MMI) were not detected by GC-MS in any of the test performed.

After 24 hours at 110 ºC, the conversion of IS reached 100 %, and surprisingly the yield of DMI was also quantitative. This result was verified by scaling up the reaction to 50 mL in a round bottom flask equipped with a reflux column at the 110 ºC, 24 h and 0.02 M. Additionally, GC-MS analysis confirmed the exclusive formation of DMI. Previous studies in the literature reported that carboxymethylated compounds such as MC and DC were the only detectable products when using acid or base catalysts under mild experimental conditions [8,10,11,47]. Only when the reaction was performed at temperatures above 200 °C, the methylated compounds become more prominent. To the best of our knowledge, this is the first time that DMI has been reported to be synthesized under mild conditions using heterogeneous basic catalysis and DMC as methylating agent.

Therefore, the first experimental parameter studied was the influence of temperature on the reaction under mild conditions and in the presence of a solid catalyst. Three temperatures (Fig. 3) were studied (90, 100, and 110 ºC). In addition, the evolution of the different intermediates formed was followed over the reaction time.

Fig. 3 illustrates that, regardless of the applied temperature, the conversion of IS was complete even at short reaction times; however, the sum of the product yields did not reach the value of 100 %. This observation, discussed in the Supplementary Information, would suggest that the compounds may be adsorbed or retained within the catalyst framework. Additionally, it can be observed that, when the reaction time was below 5 h, the predominant intermediates were MC or DC, and the formation of methylated compounds increased thereafter. For instance, after 8 h, the DMI yield reached 100 % at an applied temperature of 110 ºC (Fig. 3c), while the same yield was achieved at 100 ºC after 20 h. However, at a temperature of 90 ºC, only a 20 % DMI yield was attained after 24 h. These results confirmed that the formation of MC and DC is faster than that of the corresponding methylated compounds; MC is initially formed and then quickly transformed into DC, so the $B_{Ac}2$ mechanism does not seem to be the rate limiting step at any applied temperature.

After the thermal treatment at 450 ºC, the brucite structure collapsed and the aluminum cations remained embedded in the periclase structure of MgO, so both commercial MgO and Al_2O_3 were tested under the same experimental conditions. These catalysts were not able to direct the reaction towards DMI production after 8 h of reaction (Table S3) as the $MgAlO_x$ was able to convert the IS almost completely to DMI. The textural parameters (Table S4) of the three catalysts did not show

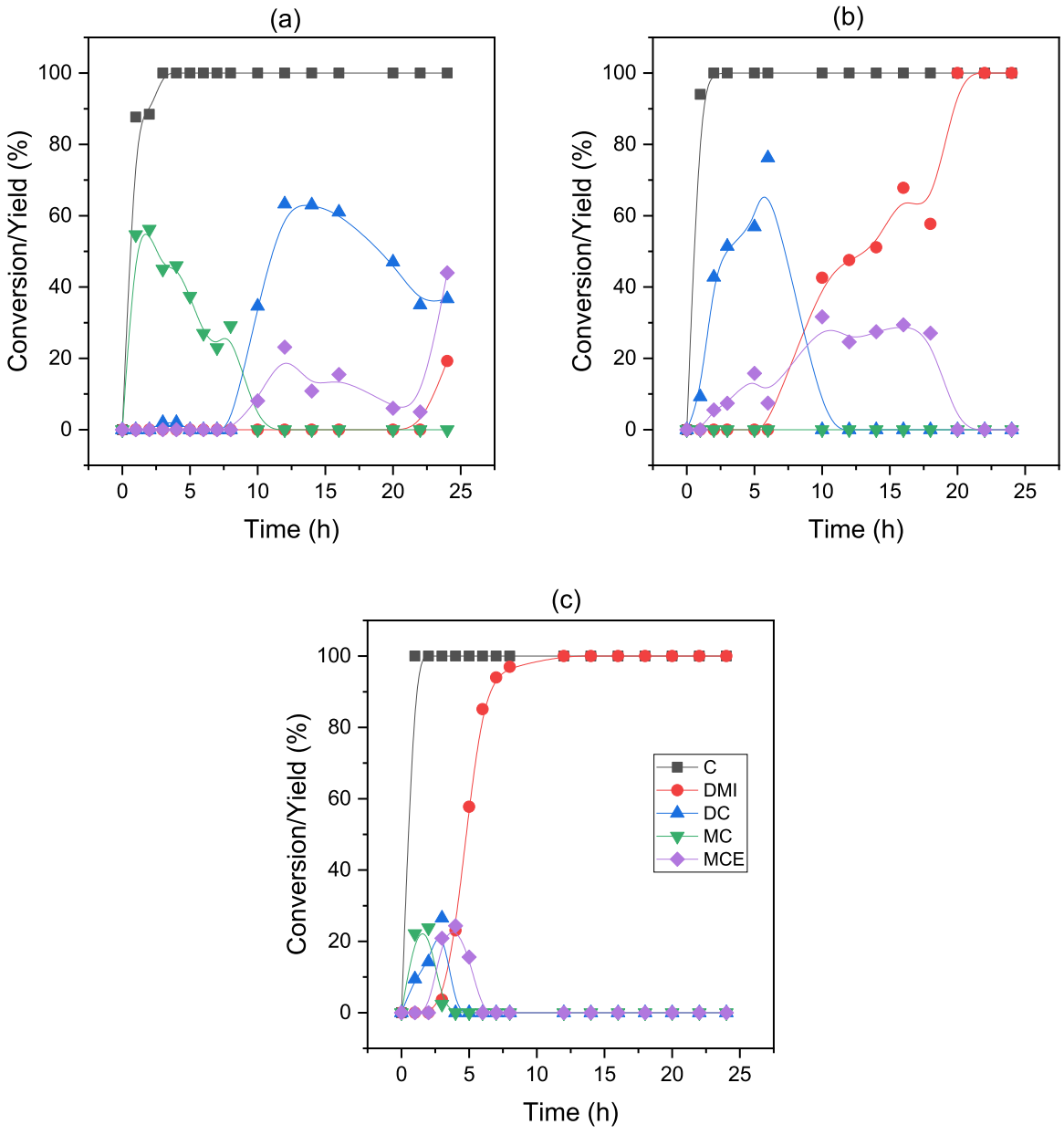

Fig. 3. IS conversion and product yields as a function of the temperature (a) 90 ºC; (b) 100 ºC and (c) 110 ºC. Experimental conditions: 100 mg of HT activated at 450 ºC; [IS] = 0.02 M; catalyst:IS mass ratio of 6.1; Volume of solution = 5 mL; atmospheric pressure.

relevant differences between them. $MgAlO_x$ catalyst showed a more pronounced microporosity than MgO or Al_2O_3, therefore it seems that the textural properties did not have an influence important enough to be considered as a key parameter controlling the activity. However, the acid (metal cations)-basic (oxide anions and Brönsted hydroxyls) properties of the catalysts seem to have a great influence on the catalytic activity. The activated hydrotalcite showed an adequate balance between the acid and basic sites, whereas the other two catalysts lack acid (MgO) or basic (Al_2O_3) sites. The basic sites are considered as centers abstracting the proton of the alcohol group of the IS, therefore the alumina showed the lowest activity to the carboxymethylated compounds, but the aluminum cation seems to play a relevant play adsorbing the carboxymethylated compounds to be further converted to DMI. These two sites are present in the activated hydrotalcite, which gives the best results for the DMI synthesis.

As anticipated, at applied temperatures below 200 ºC and in the presence of a solid catalyst, the initial stages of the reaction are predominantly governed by the $B_{Ac}2$ mechanism. However, as the reaction progresses, the formation of methylated compounds (MCE and DMI) derived from carboxymethylated derivatives becomes evident (see Fig. 3). This fact seems to indicate that the $B_{Al}2$ mechanism described for the methylation reaction does not seem to be involved in this case [48, 49], but it is rather a mechanism in which the carboxymethyl-derived compound is transformed into the methylated compound. This evidence may be due to the fact that the $B_{Al}2$ mechanism requires higher temperatures to proceed in a straightforward manner [10], as shown in the previous experiments with the flow and under autogenous pressure reactor.

To establish the key role of DC as the main intermediate in this reaction mechanism, an experiment was carried out in which a DC solution in DMC was reacted with the catalyst at the temperature of 110 °C. Results showed complete conversion of DC and 100 % selectivity towards DMI after 24 h of reaction. Notably, the conversion of DC to DMI did not occur as a result of thermal processes, as evidenced by the absence of DC conversion under similar experimental conditions without catalyst. At 200 ºC and in the presence of an activated HT, or a

basic alumina, Tundo et al. [8] reported the decarboxylation of benzylmethylcarbonate in DMC to yield the corresponding methylether (benzylmethylether) with a selectivity close to 100 % at 200 ºC. Therefore, a decarboxylation reaction seems to be involved in the conversion of DC into DMI.

The next question was whether, once DC was formed, the presence of DMC was necessary to convert DC to DMI. Therefore, further experiments were carried out to elucidate the contribution of DMC to the conversion of DC to DMI by replacing DMC with dimethylformamide (DMF) (boiling point 153 ºC) or cyclopentyl methyl ether (CPME) (boiling point 106 ºC). Consequently, the reaction was conducted with a DC concentration of 0.02 M and 100 mg of activated HT. When DMF was used as solvent, no DC conversion was observed at 110 °C, even at a temperature as high as 170 °C (above the boiling point of DMF). Similarly, with CPME, an ether with a boiling point similar to that of DMC, at 110 °C also resulted in negligible DC conversion. Taken together, these results highlight the necessary presence of the catalyst and DMC, as a reaction medium, for the successful transformation of DC to DMI. It was also verified that IS did not react with methanol in presence of the activated HT in DMF at 110 ºC; therefore, the methanol, formed during the $B_{Ac}2$ reaction, cannot be considered as potential methylating agent under these experimental conditions. In the Supplementary Information, the role of the solvent was explored in depth by studying different DMC: CPME volume ratios (Table S5), keeping the rest of the reaction parameters constant, thus completing the study on the role of DMC in the reaction. In summary, these results show that the lower the ratio DMC: CPME, the lower the DMI yield.

Finally, from the above results, it can be concluded that while the $B_{Ac}2$ mechanism is necessary for the first step of IS methylation, the next step to obtain the methylated derivatives (MCE, MMI and DMI) will not take place if both the DMC and the catalyst are not present in the medium and, therefore, a straightforward mechanism based on $B_{Al}2$ could be ruled out for the methylation of IS under the studied conditions.

3.3. Adsorption of DMC on the activated hydrotalcite

The results in batch reactors have shown that DMC is a key reagent for the DC decarboxylation to yield DMI; therefore, the adsorption of DMC on the catalyst surface was investigated by adsorption of DMC at different temperatures and evacuation times by FTIR spectroscopy analysis. Moreover, a theoretical study of FTIR spectra of the DMC adsorption at room temperature (RT) on a model solid was also carried out and compared to the observed FTIR spectra.

The spectra of the adsorbed DMC at RT and 110 ºC are shown in Figs. 4 and 5. For comparison, the spectra of methanol (MeOH) adsorbed at RT and 110 ºC are also displayed in Figure S5. In the region between 4000 and 2600 cm^{-1}, the adsorption of DMC on the $MgAlO_x$ catalyst at RT (Fig. 4) led to the appearance of a negative band centered at 3725 cm^{-1}, whereas when the adsorption is carried out at higher temperatures, a band appears at around 3745 cm^{-1}. At RT, this band was evolved with the time of DMC evacuation. Vacuum thermal treatment of the catalyst at 450 ºC does not completely dehydroxylate the $MgAlO_x$ surface (Figure S2b), as a broad band is observed in this region due to the presence of surface hydroxyl groups interacting via hydrogen bonds. However, the adsorption of DMC disturbs this band by reacting or interacting with these surface hydroxyl groups [50].

This different behavior of DMC depending on the adsorption temperature seems to indicate that, at RT, the DMC is mainly adsorbed on the surface, whereas at higher temperature it reacts with the surface, generating new hydroxyl groups. It is known that the DMC is decomposed by water into MeOH and CO_2, so the adsorbed water could catalyze such reaction [37]. The vapor phase DMC spectrum (Figure S6) in this region shows several symmetric and antisymmetric C-H bond stretching bands due to the two isomers that can occur in the gas phase [51]. These gas-phase DMC vibrations have been assigned to the asymmetric (3032 and 3004 cm^{-1}) and symmetric (2965 cm^{-1}) C-H bond stretching of the methyl groups present in the DMC. As it is shown, the spectrum of DMC in the gas phase (Figure S6) and after adsorption at RT (Fig. 4) is quite similar, whereas when adsorbed at higher temperature (Fig. 5) the spectrum is dominated by two intense bands at 2954 and 2821 cm^{-1}. In addition, two less intense bands appear at 3004 and 2866 cm^{-1}. On the other hand, when MeOH was adsorbed at RT or 110 ºC on the catalyst (Figure S5), two intense bands at 2940 and 2820 cm^{-1} are observed, which have been ascribed to the C-H stretching in the methoxide groups according to the configuration they adopt [52–55], i.e. monodentate, bidentate or bridging methoxides, pointing out that methoxy groups were formed on the surface of the catalyst after adsorption of DMC at the selected temperatures. When the adsorbed DMC was evacuated at different times, it was observed that the bands corresponding to the C-H bond gradually decreased in intensity and the

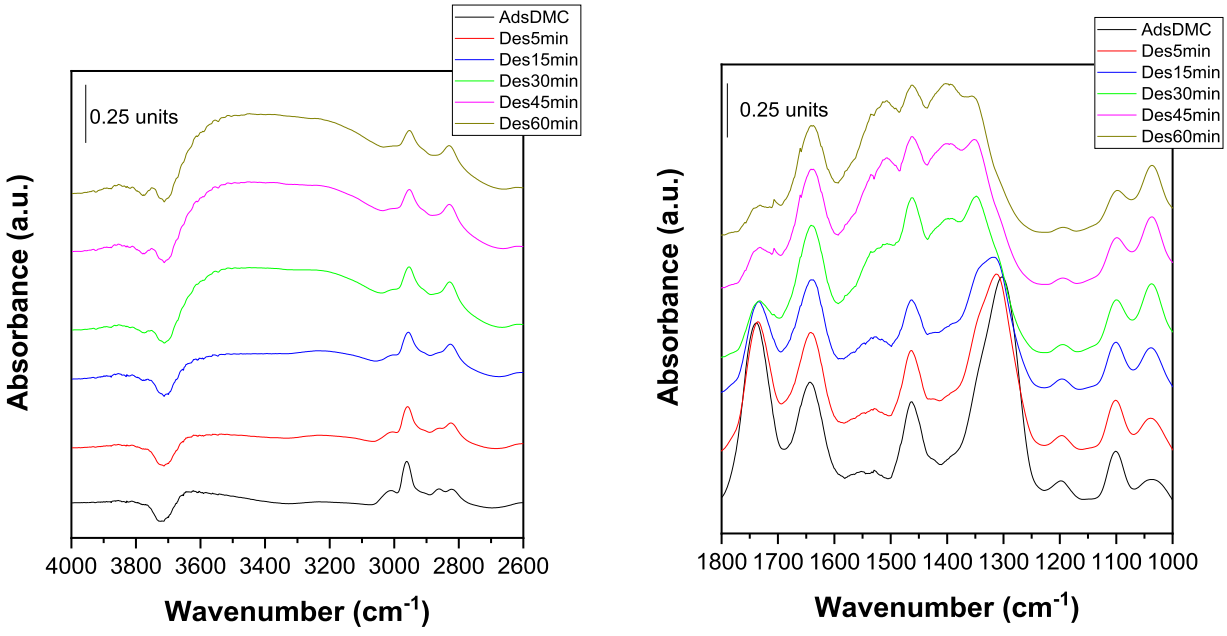

Fig. 4. FTIR analysis of the adsorption of DMC at room temperature on the surface of the activated catalyst.

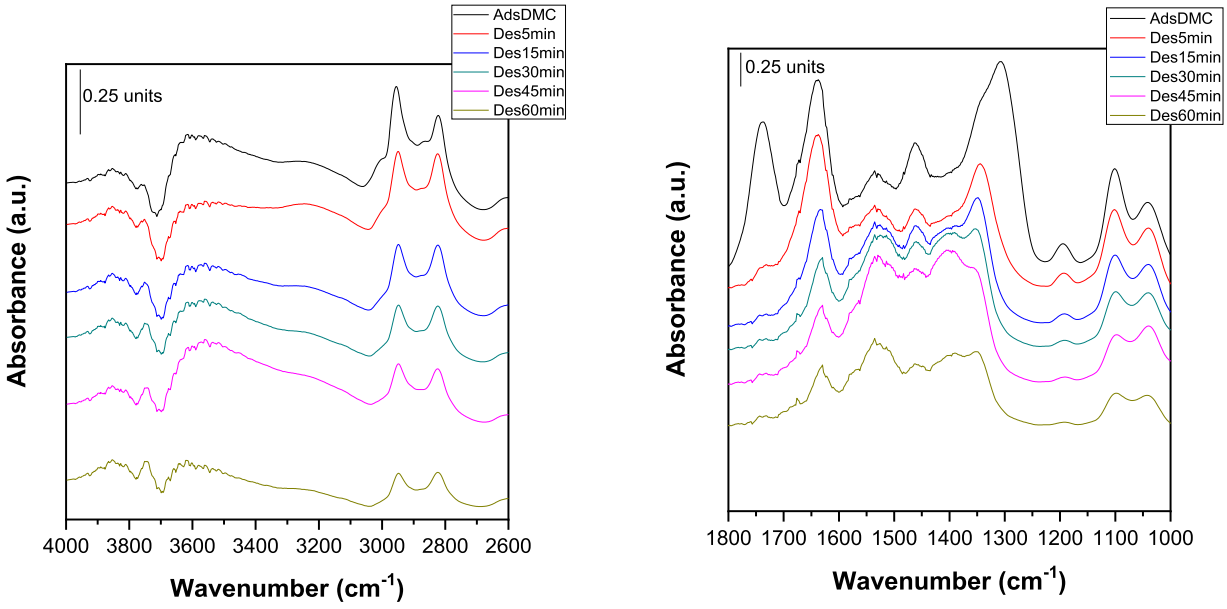

Fig. 5. FTIR analysis of the adsorption of DMC at 110 ºC on the surface of the activated catalyst.

band at 3750 cm^{-1} stood out. Also, the weak bands at 3004 and 2867 cm^{-1} disappeared with the evacuation time. Therefore, it can be concluded that DMC was mainly physisorbed, but, in addition to physisorption, DMC reacted with the catalyst surface generating adsorbed methoxide groups and other species that should present methyl groups in their structure such as monomethylcarbonate (MMC), as will be proved by the theoretical study below. This species have been reported during the thermal decomposition of DMC on different solids, such as CeO_2 [50,55], ZrO_2 [55], NaX zeolite [56], KBr/SiO_2 [57] or in the synthesis of DMC from MeOH and CO_2 [54,58–62]. This provokes, from the data presented here, that the unambiguous assignment of these vibrations to the methoxide or MMC groups is not straightforward, although it may be affirmed that both species would be present on the catalyst surface.

The presence of the methoxide and MMC groups on the catalyst surface was confirmed by the analysis of the region between 1800 and 900 cm^{-1} (Figs. 4 and 5). In this region of the spectrum, bands present in the gas-phase DMC [51] can be observed, such as those associated with the stretching vibration mode of the C═O bond (1740 cm^{-1}), the symmetric deformation of -CH_3 groups at 1460 cm^{-1} [56,58] and the band at 1310 cm^{-1} corresponding to the asymmetric O-C-O stretching [58]. In addition, there were other bands that were not present in the gas-phase DMC, such as those recorded at 1640, 1540, the shoulder at 1338 cm^{-1}, as well as the bands at 1103 and 1045 cm^{-1}. This last set of bands would be due to the methoxy groups [52–55]. Thus, that at 1103 cm^{-1} could correspond to monodentate methoxy groups [52,61–63] on different metal centers and the band at 1045 cm^{-1} to bridging methoxy groups. It should be noted that when methanol adsorption was carried out on the catalyst at 110 ºC, the most important contribution corresponds to the bridging methoxy groups (Figure S5), these being more labile when evacuated at different times. However, the theoretical study assigned the band at 1103 cm^{-1} to MMC species (*see below*) after the prediction of the IR spectrum of MMC adsorbed on the solid. These facts seem to indicate that DMC, when adsorbed on the catalyst, decomposes to form methoxy groups on the one hand and MMC on the other.

3.4. Computational studies of DMC adsorption

3.4.1. Predicted IR spectra and assignment of the IR observed bands

As a first step to check the reliability of the calculations, the calculated IR spectra of two conformers of DMC (cis-cis and trans-cis (Figure S7) hereafter DMC1 and DMC2, respectively) were compared with the observed gas-phase spectrum of our experiments (Fig. 7A). The Gibbs energy difference between both conformers is rather small (Δ_rG° = 3 kcal/mol, being DMC1 the most stable species); however, the energy barrier (Δ_aG°) for DMC1→DMC2 interconversion amounts to 10 kcal/mol. As shown in Fig. 6 A, the calculated spectra for both conformers (DMC1 and DMC2) agree quite well with the observed ones. As expected, the calculated harmonic frequencies of the normal modes are overestimated with respect to the observed bands; thus, a scale factor of 0.95 was applied to the calculated frequencies. Fig. 6B represents graphically the most intense modes associated with the observed bands given in Fig. 6 A (i), in addition, the character of each normal mode is included in the same figure. Details of the vibrational analysis are given in Tables S6-S9.

3.4.2. Adsorption of DMC on cubic magnesium oxide

The next step consists on the selection of the structural model. Thus, although the actual material is amorphous, this study was started by analyzing the adsorption of DMC1 and DMC2 on cubic magnesium oxide. On the basis of a previous work of Bonino et al. on the interaction of DMC with alkaline ions [64], it was assumed that the interaction of DMC with the alkaline earth oxide can form three types of adducts (Fig. 7): the O atom of the carbonyl moiety of DMC1 or DMC2 interacts with an metal atom of the crystal to give two types of adducts (hereafter, Up(1 or 2)-n model; n is the number of cells of the cubic MgO crystal); and the O atoms of the methoxy groups of DMC1 interact with metal atoms of the crystal to give the third type (Down-n model). These DMC-$(MgO)_x$ models are explicitly represented in Figure S8.

In a second step, the adsorption energies of the two types of DMC1 adducts and the one of DMC2 arising from the respective interactions with the (100) face of cubic MgO crystals and different cell sizes (Figure S8) were studied. The electronic adsorption energies of these systems as a function of the crystal size are represented in Figure S9, and it was found that such adsorption energies reached an asymptotic limit when the crystal contained five cells. The thermodynamic properties of 5-cells adduct obtained with the standard expressions of Statistical Thermodynamics are collected in Table S6, where it can be observed that the most stable adduct arises from the conformer DMC2. Table S6 contains the energetics of two other species that will be presented later.

Next, the attention was focused on the IR spectra of adsorbed DMC on the MgO. The calculated IR spectra of each series of the adducts of

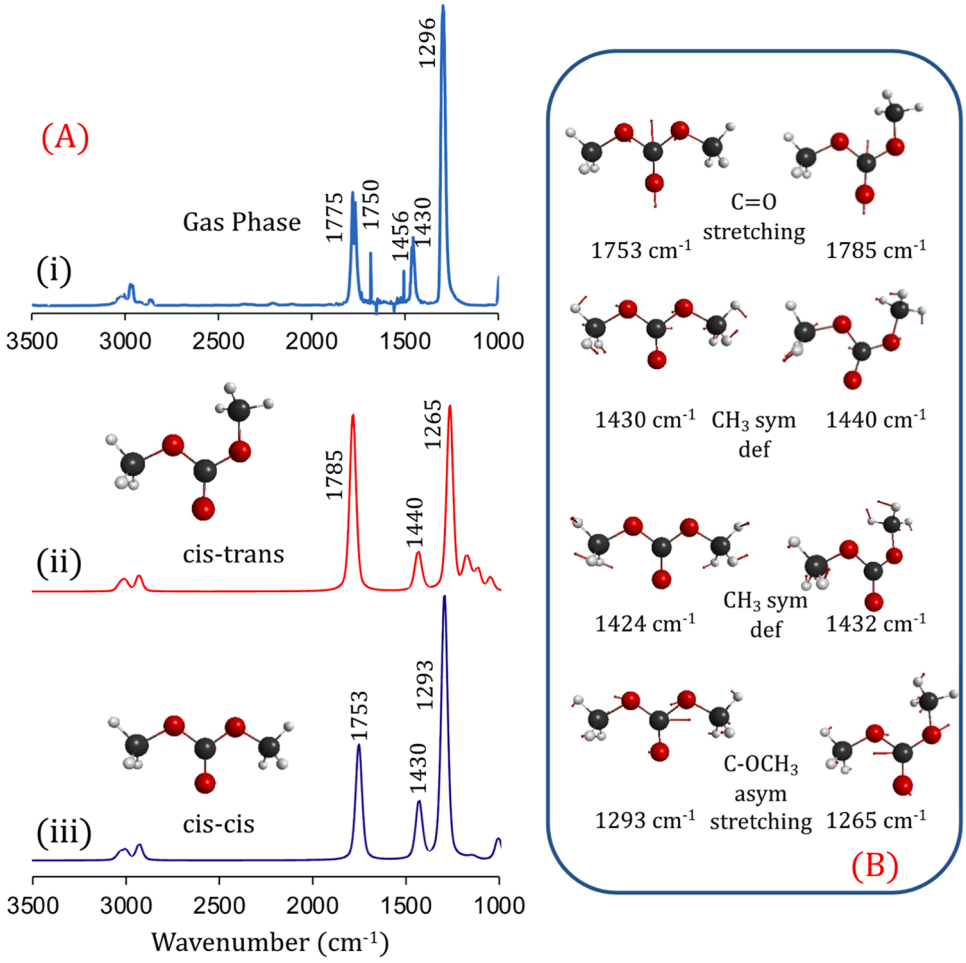

Fig. 6. (A) Experimental and calculated (M06–2X/def2-TZVPP) IR spectra of DMC. (i) Experimental (gas-phase); (ii) calculated cis-trans conformer; (iii) calculated cis-cis conformer. (B) Graphical representation of the normal modes for both conformers and vibrational assignment. The calculated spectra have been convoluted with a (0.5:0.5) Voigt function with a HWHM of 20 cm^{-1} and frequencies scaled by a factor of 0.95.

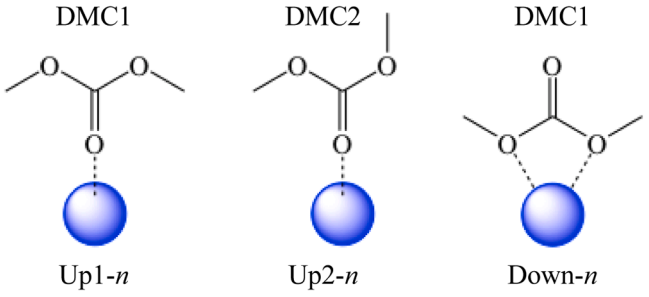

Fig. 7. Types of adsorptions of DMC on the surface of cubic MgO. (a) Up1-n; (b) Up2-n; (c) Down-n.

DMC (Figure S8) are represented in Figure S1. In contrast to energy adsorption, the general appearance of each series of spectra converges rapidly, with almost no variation from 3-cells crystals. Figure S11 represents the observed IR spectrum of DMC adsorbed on $MgAlO_x$ and the calculated IR spectra of the three types of DMC adduct models (5-cells, Figure S8). Comparison of observed and calculated spectra allows both to establish a straightforward correlation between them and the assignment of the observed spectrum. The band at 1740 cm^{-1} corresponds to ν(C═O) of the Down-n type adduct of DMC1, in which the carbonyl moiety is not bonded to the crystal surface and experiences only a small change in its frequency with respect to the free DMC1 molecule (Fig. 7). The absorption band at 1647 cm^{-1} corresponds to the ν(C═O) mode of the Up1-n and Up2-n types of adducts, and given that, in these types of adducts, the carbonyl moieties are bonded to the surface, the frequency of the mode change ~100 cm^{-1} with respect to the free molecule. The band at 1460 cm^{-1} is associated with the $\delta_{sym}(CH_3)$ of the three adducts, whereas the band at 1304 cm^{-1} and its shoulder at 1380 cm^{-1} correspond to $\nu_{as}(O\text{-}CH_3)$. Only one observed band (1101 cm^{-1}) is not explained by the above calculations, but it could be assigned to monomethyl carbonate (MMC). Figure S12 represents the calculated spectrum of MMC along with the spectrum of Up1–5 DMC, where it is observed that the bands of the two spectra overlap excepting the band that is observed in the region of 1101 cm^{-1}. Thus, the bandwidths and the above correlation suggest that four types of adsorptions are present in the experiments (three adsorptions from DMC and one from MMC).

This theoretical study has allowed to assign the bands of the spectra of the adsorbed DMC at 110 ºC, after different evacuation times, in the 1700–900 cm^{-1} region (Fig. 5). It was observed that after 5 minutes of desorption, the band at 1740 cm^{-1} disappeared, so the Down-n type adduct of DMC1 would be easily desorbed, leaving the bands corresponding to the Up1-n and Up2-n adducts and the methoxide groups. As the evacuation time increases, the intensity of the bands corresponding to these latter species gradually decreases.

Therefore, it can be concluded that DMC was strongly adsorbed on the catalyst surface through the carbonyl group, the interaction with the methoxy groups being more labile. In addition, DMC also reacts with the catalyst surface to form methoxy groups (monodentate and bridging)

and MMC, both species being stable on the catalyst surface during the reaction.

3.4.3. Adsorption of DMC on cubic mixed metal oxide

In the precedent discussion, it was feasible to explain the observed IR spectrum without the participation of the aluminum atoms, though this may lead a false impression that the role of these atoms is irrelevant. Therefore, to elucidate the function of aluminum in the catalyst, it was applied the same types of calculations to cubic crystals in which one or several magnesium atoms are randomly substituted by Al^{3+} or AlOH species (Figure S13). In Figure S13a, the IR spectra of 5-cells model for Up(1) and Down types of adsorption of DMC on Al^{3+} are represented. Although the adsorption process on Al^{3+} is strongly favored with respect to the DMC-Mg interaction, clearly, the calculated spectra cannot be correlated with the experimentally observed one. On the other hand, it was represented the spectra of the 5-cells mixed metal oxide with Up1–5 type adsorption of DMC (Figure S13b). Using this model, a good correlation between the observed and calculated spectra was obtained (Figure S13). In addition, a more favorable adsorption energy with respect to the corresponding model of pristine MgO was obtained. Therefore, the conclusions that can be extracted from these calculations are (i) DMC does not interact directly with the aluminum ions, since, if this was the case, the IR spectrum would show different appearance to that observed (Figure S13a); and (ii) the effect of the aluminum on the catalyst is to increase the adsorption energy of DMC.

3.5. Catalyst reutilization

The previous catalyst stability studies showed rapid deactivation of the catalyst whether the reaction was carried out in the flow reactor or in the reactor under autogenous pressure. An open question was whether the catalyst stability would be improved by the use of milder reaction conditions, where at least DMC decomposition would be less favored. Thus, to evaluate the catalyst reutilization, the catalytic process was performed at 110 °C in different reactors, being stopped at different reaction times (3, 6, 9 and 24 h). After each of these times, the solution was removed from the reactor and then new fresh solution was added. This procedure was conducted until five consecutive catalytic runs. This means that, for example, the catalyst in the reactor stopped at 3 h, after the fifth catalytic cycle, was working for 15 h and so on. The catalyst reused in five consecutive runs (Fig. 8) showed a drop in DMI selectivity after three cycles. On the other hand, IS conversion remained at 100 % after 5 runs, so the catalyst was not deactivated, but the selectivity pattern was changing along the catalytic runs, reaching a selectivity to DMI of 40 % after the 5th cycle. The results of the first and second catalytic cycle are quite similar, being DC the most important product at the initial stages of the reaction (9 h), which then decreased after 24 h. MCE intermediate grew until 9 h and the selectivity dropped to 0 % after 24 h. Finally, MC was only detected after 3 h for the first and second catalytic runs and the DMI yield was 100 % after 24 h.

The behavior of the catalyst for the next three catalytic runs was different from that initially observed. Now, the DC and MCE intermediates were detected throughout the catalytic run and their selectivity increased in each catalytic cycle after 24 h. Moreover, MC, which was completely converted to DC in the early hours of the reaction for the first catalytic cycles, was now detected even after 24 h at the end of the 5th cycle. It also cannot be excluded that longer reaction times could increase DMI yields beyond those observed in these experiments but the reaction was not allowed to continue beyond 24 h.

The textural properties of the catalyst after the first and fifth catalytic cycles were evaluated (Table S4). Surprisingly, the catalyst suffered a sharp decrease in specific area even after the first cycle with an almost 95 % reduction (specific area went from 82 to 4 m^2/g). This reduction was due to the blocking of the microporosity of the $MgAlO_x$ by the bulkier reaction products, such as carboxymethylates. This reduction does not appear to persist in subsequent catalytic cycles, suggesting that the micropores may no longer be accessible for carrying out the reaction in subsequent cycles. This would leave only the external surface available for the reaction. As the active centers are exposed on the surface, they are ready and available to carry out the reaction without diffusional constraints. As illustrated in Fig. 8, the DC yield exhibits an increase at the three-hour reaction time, reaching a maximum in the third cycle and subsequently declining. This suggests that as the reaction occurs on the external surface and there are no diffusional constraints, these compounds are detected in a higher proportion at the outset of the reaction. As the reuse cycles proceed, the active centers (the metal cations) become occupied by the compounds derived from the DMC, such as the methoxide groups or the MMC, and from the IS, which results in a reduction in the surface concentration of these active centers. This latter fact will ultimately cause the reactions leading to the methylated compounds to occur to a lesser extent and reduce the selectivity towards DMI as successive cycles of reuse take place. This experimental evidences emphasized that the reaction took place on the external surface of the catalyst and that the textural properties of the catalyst did not seem to play a key role in the catalytic performance, since the basic sites together with the presence of the metal cations (Lewis acid sites) on the surface of the catalyst are the actual active sites, therefore, if these sites are readily available, the reaction evolved to DMI and when they are blocked the selectivity to DMI started to decline.

Regarding the basic properties of the catalyst after the reaction, the spent catalyst exhibited a concentration of basic sites that was 44.7 μmol/g less than the initial value of 304 μmol/g. This decrease is consistent with the significant reduction in the S_{BET} of the catalyst after the reaction. However, the concentration of basic sites per square meter has increased twofold after the reaction. Given that the reaction occurred on the external surface of the catalyst, it appears that the reduction in the concentration of basic sites is offset by an increase in the density of these sites. This suggests that the reaction can proceed adequately. It is important to note that the basic sites are involved in the initial reaction step of the mechanism, whereby they activate the isosorbide by abstracting a proton from the alcohol group. Consequently, if the basic sites are readily available, the initial step will proceed.

In any case, these results show that the catalyst surface underwent changes that influenced on the selectivity patterns, which could be related to the adsorption of reactants or intermediates on the catalyst surface. Therefore, the catalyst was characterized after the fifth run by means of several analytical techniques in order to evaluate the causes of such selectivity changes.

First, the catalysts were analyzed by elemental analysis to detect the amount of carbonaceous deposits formed after the fifth cycle of each reaction time (Table 1). As expected, the amount of carbon increased with the reaction time, although the catalyst after 6 h displayed the highest amount of carbon (Table 1), the differences between them are quite small.

In order to understand the nature of the adsorbed species, thermogravimetric analysis was carried out for each catalyst along with fresh $MgAlO_x$. In general, the weight losses (Table 1) increased slightly with the reaction time, according to the CNH results. On the other hand, the catalyst after 6 hours showed the highest weight loss.

On the other hand, when the heat flows were compared as a function of the reaction time (Figure S16a), it is noteworthy that the shape of the curves was quite similar regardless of the time that the catalyst has been used for. This suggests that the adsorbed species after each reaction time should have a similar structure, otherwise dissimilar plots should be expected. On the other hand, these plots are not similar to that of fresh $MgAlO_x$. This catalyst did not show an exothermic peak in the corresponding DTA curve, but rather an endothermic band was detected, which should be due to a decarbonation process of the catalyst. It must be highlighted that the $MgAlO_x$ catalyst after several days in contact with the laboratory atmosphere was not active in the reaction (no IS conversion at all), which is strong evidence that the carbonation is a deactivating process and not the main cause of the selectivity changes, i.

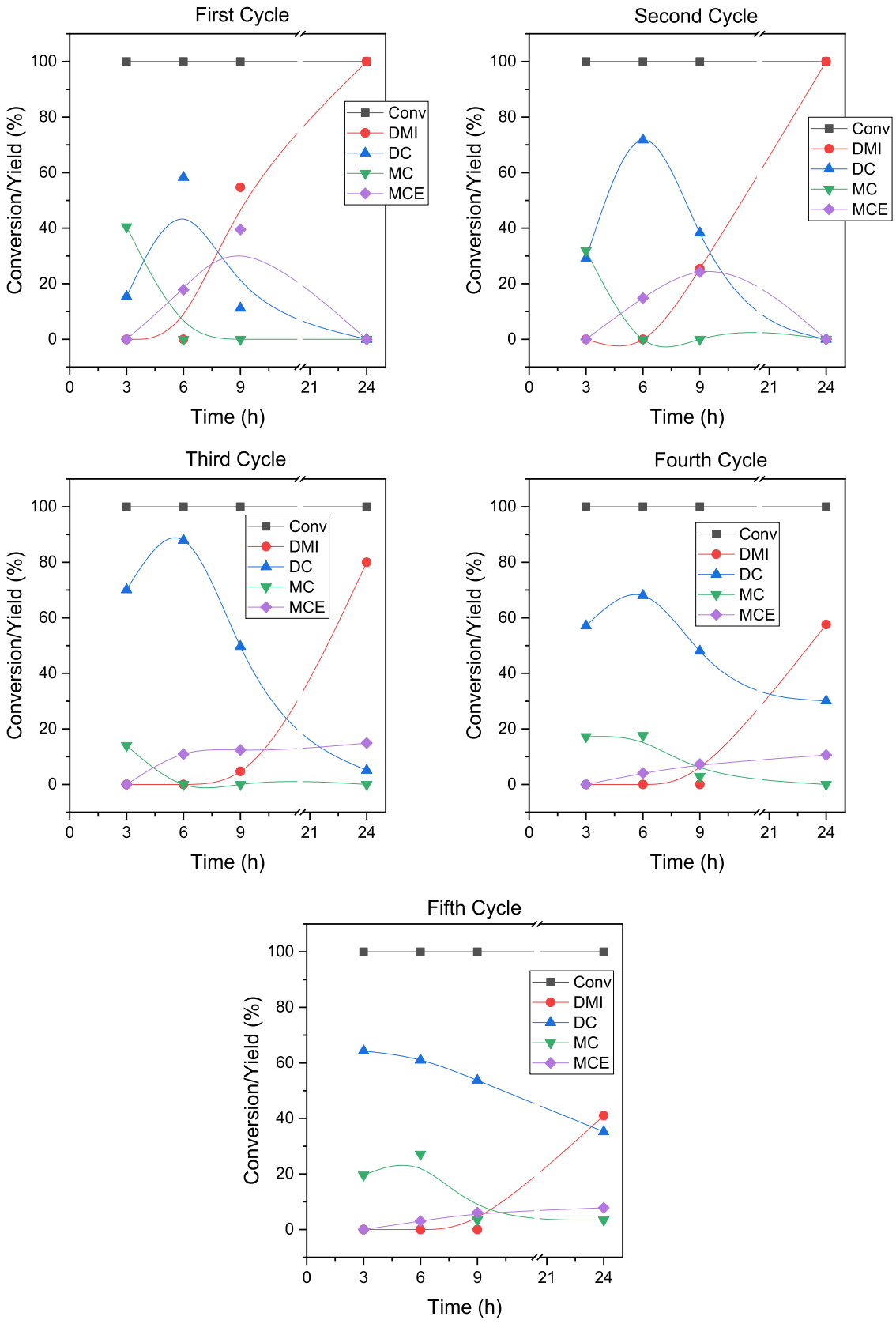

Fig. 8. Catalyst reutilization. Experimental conditions for each catalytic cycle: [IS] = 0.02 M; 100 mg of HT activated at 450 °C; Volume of solution = 5 mL; atmospheric pressure; T = 110 °C.

Table 1
Elemental analysis of the catalyst after the fifth catalytic run and weight loss determined by TG analysis.

Time[a] (h)	C (%)	H (%)	Weight loss[b] (%)
3	2.25	1.21	19.6
6	2.97	1.21	20.9
9	2.32	1.26	20.5
24	2.75	1.13	20.0

[a] The number indicates that the reactor was stopped at such time and after the 5th catalytic run;
[b] Determined from the TG analysis

e., if carbonation takes place, the conversion of IS will decrease continuously and this fact is not observed at all.

The gases evolved during the thermal analysis were analyzed by mass spectroscopy (Figure S16b) and it is noted that the CO_2 and H_2O signals are due to the burned organic matter adsorbed on the catalysts, but they are not associated with a decarbonation process, since the DTA curve displays a clear exothermic peak at roughly 285 ºC. In addition, the CO_2 mass signal for each temperature tested shows a shape similar to those of DTA plots, confirming that the adsorbed species should have an analogous composition and structure regardless of the reaction time.

In order to gain a deeper insight into the nature of carbonaceous deposits on the catalyst surface, both ^{13}C and ^{1}H-ss NMR analyses of the used catalyst were carried out after the 5th run at 24 h. For comparison and to understand the spectral features of the reused catalyst, the ^{13}C and ^{1}H-ss NMR analyses were also performed of the $MgAlO_x$ catalyst after several weeks in contact with the atmosphere, as well as of $MgAlO_x$ in contact with DMC at 110 ºC and after 24 h and, finally, the ^{13}C-ss NMR analysis of DC was also recorded as an example of IS-derived compound. These spectra are shown in Fig. 9.

The assignment of the ^{13}C bands (Fig. 9a) is not straightforward, because of the possible compounds that could be adsorbed on the surface of the solid. However, some conclusions can be drawn after comparing the different spectra:

1) The $MgAlO_x$ catalyst in contact with the atmosphere show a signal at 170 ppm which has been observed for inorganic carbonates, such as $MgCO_3$ [65–68].
2) After contacting $MgAlO_x$ with DMC at 110 ºC for 24 h, two peaks are observed: one at the same position as the carbonate group for the catalyst in contact with the atmosphere (170 ppm) and another one

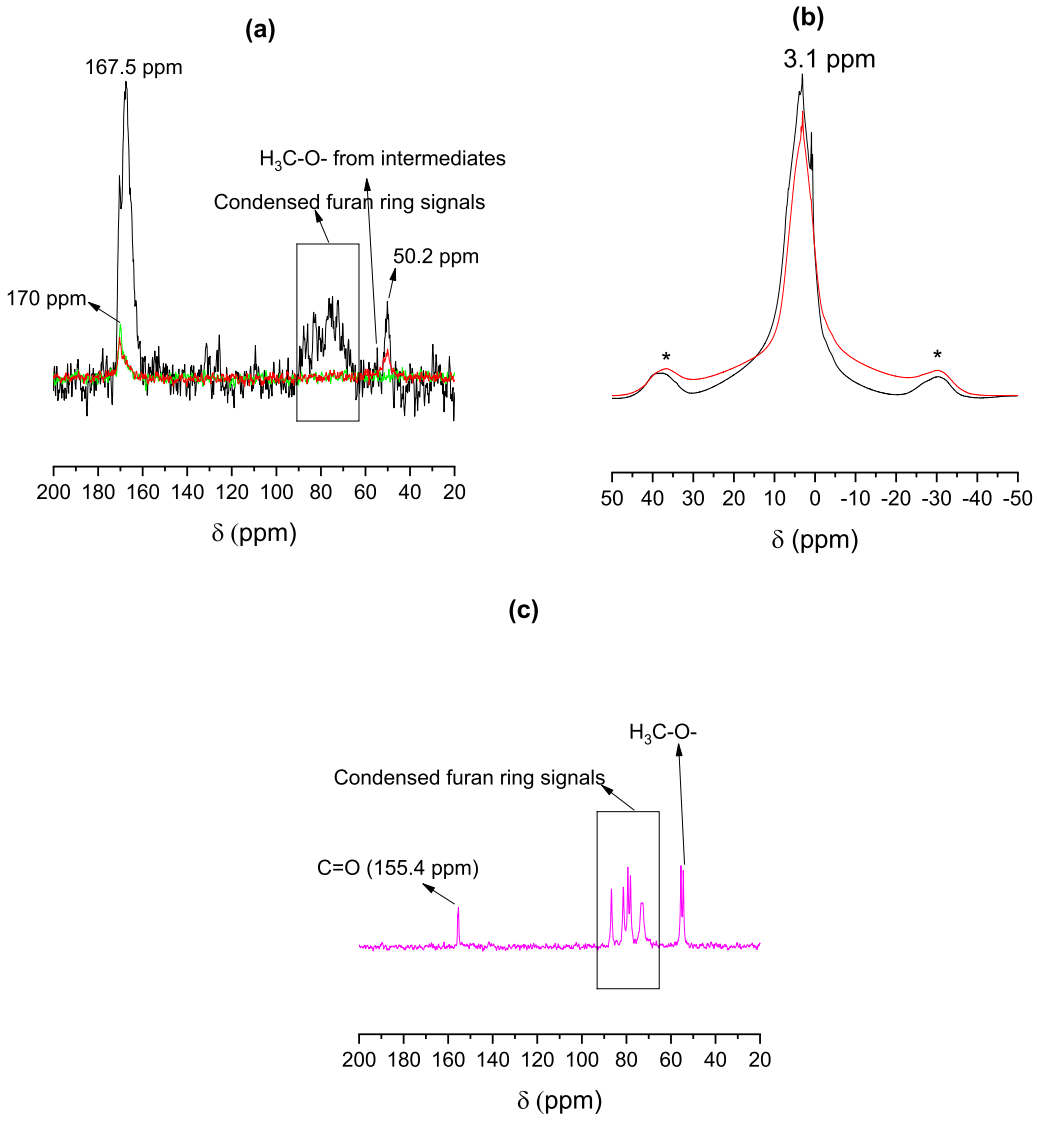

Fig. 9. (a) ^{13}C-ss NMR of the catalyst after 5 cycles of reutilization and 24 hours each cycle (black line). In green, the $MgAlO_x$ solid in contact with the atmosphere and in red the $MgAlO_x$ solid in contact with the DMC. (b) ^{1}H-ss NMR of the catalyst after 5 cycles of reutilization and 24 hours each cycle. In red, the $MgAlO_x$ solid in contact with the DMC. (c) ^{13}C-ss NMR spectrum of DC compound.

at 50.2 ppm. In this case, the first one would be ascribed to the carbonyl group of adsorbed DMC, while the second peak could be assigned to methoxy groups as a result of the decomposition of the DMC on the catalyst surface, as FTIR spectroscopy analysis of the adsorbed DMC showed. The methoxy group signal for liquid DMC lies on 53 ppm [69], so this would be another evidence of the decomposition of DMC on the catalyst surface. The ^{1}H-ssNMR analysis (Fig. 9b) showed a peal at 3.1 ppm, corresponding to the adsorbed methoxy groups, though this is quite broad, and the inclusion of the signals corresponding to the IS intermediates in this signal cannot be rule out.

3) The spectra of DC (Fig. 9c) showed signals at 55 ppm, between 73 and 87 ppm and at 155 ppm, which can be assigned to the methoxy group of the carboxymethoxy moieties, to the condensed furanic rings and the carbonyl groups, respectively [10].
4) Finally, the reused catalyst showed all those spectral features, both those associated with the decomposition of DMC (170 and 50.2 ppm) and those due to the adsorption of IS-derived compounds (167.5, 90–70 and 55 ppm). The chemical shift of the carbonyl signal to higher field would be indicative of the interaction through the carbonyl group between the IS intermediates and the catalyst surface.

Therefore, from these experimental evidences, it can be concluded that the change in the pattern selectivity of the catalyst was due to the fact that the surface of the reused catalyst was covered by multiple compounds, resulting in a reduction in the number of active sites, leading to a lower capacity to conduct the methylation of the hydroxyl groups of the IS. Presumably, adsorbed methoxide groups generated from DMC adsorption and bonded to metal cation centers could be the species most influencing the selectivity pattern of the reused catalyst, since each adsorbed intermediate was evolving to the corresponding compound as the reaction proceed, whereas the FTIR spectroscopy analysis (Fig. 5) showed that methoxy species were not evacuated from the surface at the reaction temperature.

3.6. Discussion

These catalytic results point out that DMI synthesis can be achieved in flow or batch processes, in the presence of a basic catalyst. In the former case, the formation of DMI requires more severe experimental conditions, such as higher pressure and temperature, reaching a 40 % DMI yield after 1 h, although the yield decreases significantly for longer reaction time. Under batch conditions, both at autogenous and atmospheric pressure, the yields are higher, but require longer reaction times. Surprisingly, the reaction in a reactor at atmospheric pressure and at the temperature of 110 °C allowed to reach 100 % yield at DMI after 8 h reaction.

Experiments carried out at atmospheric pressure using the DC intermediate have shown that the presence of both the DMC and the catalyst are necessary for the reaction to proceed, and that the absence of either of them prevents the formation of DMI. Therefore, the decarboxylation of DC to produce DMI would involve a mechanism in which either the DMC or the DC, or both, must be activated by the catalyst. Adsorption studies of DMC followed by FTIR spectroscopy analysis have demonstrated that DMC reacts with the catalyst surface generating two adsorbed compounds, methoxy groups and the monomethylated derivative of DMC (MMC). In addition, the study of the used catalyst also evidenced the adsorption of the carboxymethylated IS derivatives. The adsorption of both DMC and IS derivatives can be expected to occur via the carbonyl group, as shown by theoretical calculations. Once these compounds are adsorbed and activated on the catalyst, an interaction between them should be expected to occur, which generates the methylated IS derivatives (MCE, MMI and DMI) and these are desorbed from the catalyst surface. This is inferred from the absence of the FTIR bands associated with the methylated compounds when the catalyst is analyzed after different reaction times.

The adsorption of the DMC via the carbonyl group onto a metal center of the catalyst should shift the charge from the methyl groups to the carbonyl oxygen, generating a positively charged center on the methyl groups of DMC. This may make the attack on the methyl groups from the carboxymethyl group of the DC (or MC) more favorable.

This is finally summarized in the following proposed mechanism (Scheme 2) for the basic heterogeneous catalytic synthesis of DMI. It should be noted that Scheme 2 shows the formation of MMI instead of DMI, for the sake of clarity and to avoid many compounds in the Scheme and complicate the understanding of the mechanism:

Step 1: The hydrogen from one of the alcohol groups of the IS is extracted by a basic center of the catalyst, i.e., surface oxide groups, since the low acidity of alcohol groups requires strong basic sites to extract the proton from the alcohol.

Step 2: The alkoxide group previously generated (hard base according to Pearson's theory) attacks the carbonyl group of DMC (hard acid according to Pearson's theory) by a $B_{Ac}2$ mechanism, generating the carboxymethylated compound MC. This reaction is most likely expected to take place under homogeneous conditions, between the activated IS and the DMC, due to the excess of DMC over the adsorbed DMC. The Scheme 2 shows in the step 3 the adsorption of MC on the surface and its final evolution to MMI but, probably the hydroxyl group of the MC will lose the proton as in the step 1 and then it will attack another DMC molecules generating the DC because the formation of MMI was not observed by the analytical analysis. Therefore, the Scheme 2 shows the evolution from IS to MMI for the sake of clarity. On the other hand, the generated methoxide group can be adsorbed on a metal center, as inferred from FTIR spectroscopy analysis. Thus, in these first two steps of the reaction, the role of the catalyst is to activate the IS to make the alcohol group more nucleophilic and attack the carbonyl group of DMC.

Step 3: As the absence of the DMC or the catalyst causes the reaction to stop at the carboxymethylated products, the DMC and/or the IS-derived compound (MC or DC) in step 2 must be activated by the catalyst, via the interaction between the carbonyl group and the cationic metallic center of the catalyst.

The methyl groups (marked in red) of the activated DMC on the catalyst would have a charge defect that would make them prone to be attacked by the oxygen IS-carboxylated compound, so that this oxygen would be positively charged.

Step 4: Finally, the compound derived from the IS in step 3 would undergo an attack on the carbonyl group by the traces of water in the medium, releasing the monomethylated compound (MMI) or the dimethyl derived compound (DMI) from the IS.

This proposed mechanism is consistent with the experimental evidence observed in the various tests. It shows that, as the reaction progresses, the catalyst surface is covered with the by-products generated by the reaction (methoxy groups in step 2 of the mechanism and DMC derivatives in steps 3 and 4 of the mechanism), which would explain why, as the catalyst is recycled, the more abundant compounds are carboxymethylated and the formation of methylated compounds is reduced, since the former would be prevented from adsorbing on the catalyst surface and therefore cannot evolve into methylated compounds. The adsorption of these compounds would also confirm what was observed by thermal and elemental analysis, where no differences were observed when the catalyst was analyzed at different reaction times and catalytic cycles, leading to the conclusion that the nature of the compounds adsorbed should be similar. Another phenomenon that this mechanism also shows is that the formation of CO_2 is not necessary, since the attack of the IS on the DMC by means of a $B_{Al}2$ mechanism does not take place. Therefore, if CO_2 were formed, it would react with the basic groups of the catalyst, deactivating them and thus avoiding the first stage of the mechanism, and with that the SI conversion would decrease with the reaction time or with the reuse cycles, but what is observed is that the SI conversion is always 100 %, regardless of the reaction conditions and the reuse cycle of the catalyst.

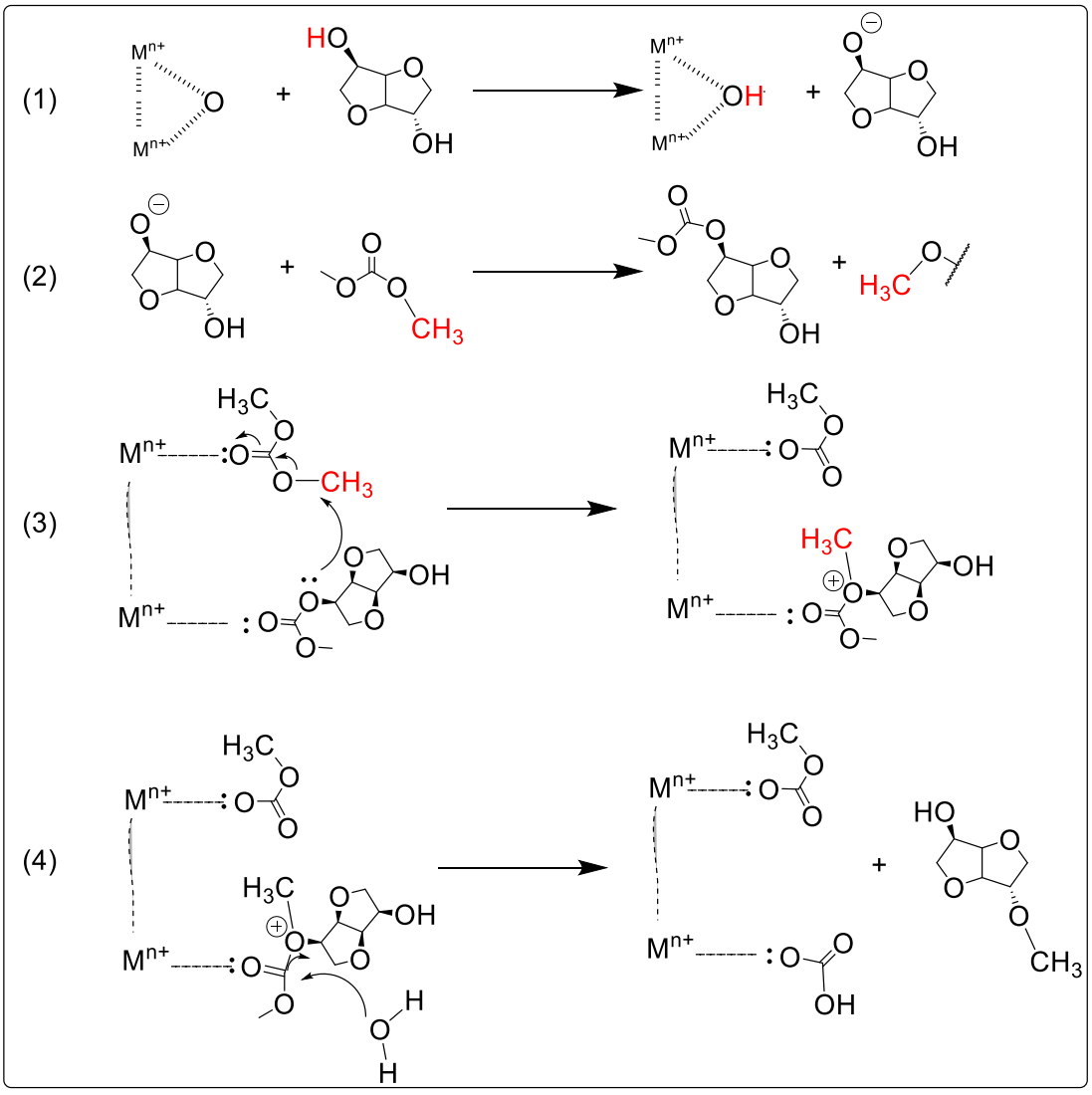

Scheme 2. Proposessd mechanism for MMI formation, showing the role of catalyst and DMC.

In case the temperature is high enough, the $B_{Al}2$ mechanism can be operating, in which the alkoxide group generated in step 1 would attack the methyl group of DMC, directly generating the methylated derivative, CO_2 and MeOH. This is what would be observed under the conditions tested in the flow reactor and in the batch reactor at high temperature.

4. Conclusions

This work has demonstrated that the synthesis of DMI can be achieved both in a flow and batch reactor. However, in a flow reactor, the maximum DMI yield was 37 % after 67 minutes of reaction at 200 ºC. This yield was improved when switching to a batch reactor, with the best results being achieved for the case where the reactor was working under atmospheric pressure conditions versus the reactor under autogenous pressure. In the first case, the yield was 100 % at 110 ºC, after 8 h of reaction, while in the case of the second one, it was 70 %, at 200 ºC after 24 h. In the three cases studied, there is a change in the selectivity to the different reaction products as the catalyst either increases its working time (flow reactor) or is reused in several catalytic cycles (batch reactors), decreasing the selectivity to DMI continuously.

Since the batch reactor gave the best results under milder reaction conditions, a study of how different parameters affected the reaction was carried out. It was observed that the transformation from DC to DMI was not a thermal reaction, but required the presence of both DMC and catalyst. This fact has led to propose a mechanism in which both the DMC and the carboxymethylated intermediates were adsorbed and activated on the catalyst surface, later evolving to DMI. The activation of both compounds can be deduced from computational studies of DMC adsorption on the catalyst, which showed that DMC adsorbs preferentially on the Al cation via the carbonyl group, as opposed to adsorption by the methoxy group. Therefore, it is expected that the carboxymethylated compounds also interact with the catalyst via the carbonyl group of the carbonate.

The changes observed in the selectivity pattern of the catalyst during its reuse in the reactor at atmospheric pressure are due to the presence on its surface of compounds derived from DMC, such as methoxy groups and MMC, which cover the active centers of the catalyst, preventing the DC formed from evolving to DMI.

CRediT authorship contribution statement

Manuel López-Granados: Resources, Methodology, Investigation. **Juan Soto:** Writing – review & editing, Writing – original draft, Methodology, Investigation, Funding acquisition, Conceptualization. **Ramon Moreno-Tost:** Writing – review & editing, Writing – original draft, Validation, Supervision, Project administration, Methodology,

Investigation, Funding acquisition. **Giacomo Trapasso:** Writing – review & editing, Methodology, Investigation. **Fabio Aricò:** Writing – review & editing, Resources, Methodology, Investigation. **José Santamaría-González:** Writing – review & editing, Methodology, Investigation, Conceptualization. **Pedro Maireles-Torres:** Writing – review & editing, Project administration, Methodology, Investigation, Funding acquisition, Conceptualization. **María José Ginés-Molina:** Writing – original draft, Methodology, Investigation, Data curation. **Juan Antonio Cecilia-Buenestado:** Writing – review & editing, Validation, Data curation. **Rafael Luque:** Writing – review & editing, Resources, Methodology, Conceptualization.

Declaration of generative AI and AI-assisted technologies in the writing process

During the preparation of this work RMT used DeepL Write in order to improve the English readability of the manuscript and for revising the grammar of the manuscript. After using this DeepL Write, RMT reviewed and edited the content as needed and take full responsibility for the content of the publication.

Declaration of Competing Interest

The authors declare that they have no known competing financial interests or personal relationships that could have appeared to influence the work reported in this paper

Acknowledgments

This research was funded by the Spanish Ministry of Science and Innovation (PID2021- 122736OB-C42), FEDER (European Union) funds (PID2021–122736OB-C42, FQM-155). Juan Soto thanks the Spanish Ministry of Science and Innovation (MCIN/AEI/10.13039/501100011033) through project PID2021–122613OB-I00. The work conducted by F. Aricò and G. Trapasso was supported by the DoE 2023–2027 (MUR, AIS.DIP.ECCELLENZA2023_27.FF project). RMT thanks the University of Málaga/CBUA for funding the open access charge.

Appendix A. Supporting information

Supplementary data associated with this article can be found in the online version at doi:10.1016/j.apcata.2024.120088.

Data availability

Data will be made available on request.

References

[1] R.A. Sheldon, J. Mol. Catal. A. Chem. 422 (2016) 3–12.
[2] J. Iwanejko, E. Wojaczynska, T.K. Olszewski, Curr. Opin. Green. Sustain. Chem. 10 (2018) 27–34.
[3] S.H. Pyo, J.H. Park, T.S. Chang, R. Hatti-Kaul, Curr. Opin. Green. Sustain. Chem. 5 (2017) 61–66.
[4] A.H. Tamboli, A.A. Chaugule, H. Kim, Chem. Eng. J. 323 (2017) 530–544.
[5] H.Z. Tan, Z.Q. Wang, Z.N. Xu, J. Sun, Y.P. Xu, Q.S. Chen, Y. Chen, G.C. Guo, Catal. Today 316 (2018) 2–12.
[6] M. Selva, A. Perosa, Green. Chem. 10 (2008) 457–464.
[7] F. Aricò, A.S. Aldoshin, P. Tundo, ChemSusChem 10 (2017) 53–57.
[8] P. Tundo, S. Memoli, D. Hérault, K. Hill, Green. Chem. 6 (2004) 609–612.
[9] F. Aricó, U. Toniolo, P. Tundo, Green. Chem. 14 (2012) 58–61.
[10] P. Tundo, F. Aricò, G. Gauthier, L. Rossi, A.E. Rosamilia, H.S. Bevinakatti, R. L. Sievert, C.P. Newman, ChemSusChem 3 (2010) 566–570.
[11] J.R. Ochoa-Gómez, L. Lorenzo-Ibarreta, C. Diñeiro-García, O. Gómez-Jiménez-Aberasturi, RSC Adv. 10 (2020) 18728–18739.
[12] M.D. Zenner, Y. Xia, J.S. Chen, M.R. Kessler, ChemSusChem 6 (2013) 1182–1185.
[13] W. Fang, Y. Zhang, Z. Yang, Z. Zhang, F. Xu, W. Wang, H. He, Y. Diao, Y. Zhang, Y. Luo, Appl. Catal. A Gen. 617 (2021) 118111.
[14] H. Kobayashi, H. Yokoyama, B. Feng, A. Fukuoka, Green. Chem. 17 (2015) 2732–2735.
[15] O.A. Rusu, W.F. Hoelderich, H. Wyart, M. Ibert, Appl. Catal. B Environ. 176–177 (2015) 139–149.
[16] S. Yang, X. Yang, X. Meng, L. Wang, Green. Chem. 24 (2022) 4082–4094.
[17] M. Annatelli, D. Dalla Torre, M. Musolino, F. Aricò, Catal. Sci. Technol. 11 (2021) 3411–3421.
[18] F. Russo, F. Galiano, F. Pedace, F. Aricò, A. Figoli, ACS Sustain. Chem. Eng. 8 (2020) 659–668.
[19] F. Aricò, P. Tundo, Beilstein J. Org. Chem. 12 (2016) 2256–2266.
[20] D. Dalla Torre, M. Annatelli, F. Aricò, Catal. Today 423 (2023) 1–10.
[21] M.I.N.E.C.F.A. Perrard, Method for Preparing Dialkyloxydianhyrohexitol by Etherification of Dianhydrohexitol Using a Light Alcohol, Presence Acidic Catal. (2015).
[22] M.C. Duclos, A. Herbinski, A.S. Mora, E. Métay, M. Lemaire, ChemSusChem 11 (2018) 547–551.
[23] P. Che, F. Lu, X. Si, J. Xu, RSC Adv. 5 (2015) 24139–24143.
[24] J.F. Arenas, J. Soto, D. Pelaez, D.J. Fernandez, J.C. Otero, Int. J. Quantum Chem. 104 (2005) 681–694.
[25] Y. Zhao, D.G. Truhlar, Theor. Chem. Acc. 120 (2008) 215–241.
[26] J. Soto, J. Phys. Chem. A 127 (2023) 9781–9786.
[27] F. Weigend, R. Ahlrichs, Phys. Chem. Chem. Phys. 7 (2005) 3297–3305.
[28] F. Weigend, Phys. Chem. Chem. Phys. 8 (2006) 1057–1065.
[29] D.J. Frisch, M.J.; Trucks, G.W.; Schlegel, H.B.; Scuseria, G.E.; Robb, M.A.; Cheeseman, J.R.; Scalmani, G.; Barone, V.; Petersson, G.A.; Nakatsuji, H.; Li, X.; Caricato, M.; Marenich, A.V.; Bloino, J.; Janesko, B.G.; Gomperts, R.; Mennucci, B.; Hratch, Gaussian, Inc., Wallingford CT (2016).
[30] B.M. Bode, M.S. Gordon, J. Mol. Graph. Model. 16 (1998) 133–138.
[31] G. Schaftenaar, J.H. Noordik, J. Comput. Aided Mol. Des. 14 (2000) 123–134.
[32] J.F. Arenas, S.P. Centeno, J.I. Marcos, J.C. Otero, J. Soto, J. Chem. Phys. 113 (2000) 8472–8477.
[33] J.C.D. and P.C.C.] E. B. Wilson, Jr., Molecular Vibrations, McGraw-Hills, New York, NY, 1955.
[34] J. Soto, D. Peláez, M. Algarra, J. Chem. Phys. 158 (2023).
[35] R. Maderuelo-Solera, A.L. Ledesma-Muñoz, C. García-Sancho, J.A. Cecilia, A. Infantes-Molina, J. Mérida-Robles, P. Maireles-Torres, R. Moreno-Tost, Catal. Today 421 (2023) 114197.
[36] S.G. Newman, K.F. Jensen, Green. Chem. 15 (2013) 1456–1472.
[37] Y. Fu, H. Zhu, J. Shen, Thermochim. Acta 434 (2005) 88–92.
[38] P. Tundo, F. Aricò, ChemSusChem 16 (2023).
[39] S.S. Ravuru, A. Jana, S. De, Sep. Purif. Technol. 277 (2021) 119631.
[40] J. Kuljiraseth, A. Wangriya, J.M.C. Malones, W. Klysubun, S. Jitkarnka, Appl. Catal. B Environ. 243 (2019) 415–427.
[41] R. Cueff, G. Baud, M. Benmalek, J.P. Besse, J.R. Butruille, M. Jacquet, Surf. Coat. Technol. 80 (1996) 96–99.
[42] A.H. Padmasri, A. Venugopal, V. Durga Kumari, K.S. Rama Rao, P. Kanta Rao, J. Mol. Catal. A Chem. 188 (2002) 255–265.
[43] Z. Jin, Y. Jia, K.S. Zhang, L.T. Kong, B. Sun, W. Shen, F.L. Meng, J.H. Liu, J. Alloy. Compd. 675 (2016) 292–300.
[44] G. Xiao-hong, C. Guang-hao, S. Chii, J. Environ. Sci. 19 (2007) 438–443.
[45] G.P. López, D.G. Castner, B.D. Ratner, Surf. Interface Anal. 17 (1991) 267–272.
[46] F.C. Liu, P. Dong, W. Lu, K. Sun, Appl. Surf. Sci. 466 (2019) 202–209.
[47] S. Jin, A.J. Hunt, J.H. Clark, C.R. McElroy, Green. Chem. 18 (2016) 5839–5844.
[48] M. Selva, Pure Appl. Chem. 79 (2007) 1855–1867.
[49] P. Tundo, M. Selva, Acc. Chem. Res. 35 (2002) 706–716.
[50] S.Y. Zhao, S.P. Wang, Y.J. Zhao, X.Bin Ma, Chin. Chem. Lett. 28 (2017) 65–69.
[51] B. Collingwood, H. Lee, J.K. Wilmshurst, Aust. J. Chem. 19 (1966) 1637–1649.
[52] I. Prymak, O. Prymak, J. Wang, V.N. Kalevaru, A. Martin, U. Bentrup, S. Wohlrab, ChemCatChem 10 (2018) 391–394.
[53] G. Hincapié, D. López, A. Moreno, Catal. Today 302 (2018) 277–285.
[54] B. Liu, C. Li, G. Zhang, X. Yao, S.S.C. Chuang, Z. Li, ACS Catal. 8 (2018) 10446–10456.
[55] L. Chen, S. Wang, J. Zhou, Y. Shen, Y. Zhao, X. Ma, RSC Adv. 4 (2014) 30968–30975.
[56] N. Tilman, J. Chem. Soc. - Faraday Trans. 94 (1998) 985–993.
[57] B. Chen, Q. Dong, N. Zhao, W. Wei, Y. Sun, J. Chem. Soc. Pak. 31 (2009) 552–558.
[58] S.T. King, J. Catal. 538 (1996) 530–538.
[59] K. Tomishige, Y. Ikeda, T. Sakaihori, K. Fujimoto, J. Catal. 192 (2000) 355–362.
[60] K.Taek Jung, A.T. Bell, J. Catal. 204 (2001) 339–347.
[61] M. Bensitel, V. Moraver, J. Lamotte, O. Saur, J.C. Lavalley, Spectrochim. Acta - Part A Mol. Spectrosc. 43 (1987) 1487–1491.
[62] J. Engeldinger, C. Domke, M. Richter, U. Bentrup, Appl. Catal. A Gen. 382 (2010) 303–311.
[63] S. Rousseau, O. Marie, P. Bazin, M. Daturi, S. Verdier, V. Harlé, J. Am. Chem. Soc. 132 (2010) 10832–10841.
[64] F. Bonino, A. Damin, S. Bordiga, M. Selva, P. Tundo, A. Zecchina, Angew. Chem. - Int. Ed. 44 (2005) 4774–4777.
[65] J.A. Surface, P. Skemer, S.E. Hayes, M.S. Conradi, Environ. Sci. Technol. 47 (2013) 119–125.
[66] J.K. Moore, J.A. Surface, A. Brenner, P. Skemer, M.S. Conradi, S.E. Hayes, Environ. Sci. Technol. 49 (2015) 657–664.
[67] H.W. Papenguth, R.J. Kirkpatrick, B. Montez, P.A. Sandberg, Am. Mineral. 74 (1989) 1152–1158.
[68] A. Lund, G.V. Manohara, A.Y. Song, K.M. Jablonka, C.P. Ireland, L.A. Cheah, B. Smit, S. Garcia, J.A. Reimer, Chem. Mater. 34 (2022) 3893–3901.
[69] S. Khokarale, T. Bui, J.-P. Mikkola, Sustain. Chem. 1 (2020) 298–314.